8828 *Inorg. Chem.* **2010**, *49*, 8828–8847
DOI: 10.1021/ic1009913

Inorganic Chemistry
Article

New [2 × 2] Copper(I) Grids as Anion Receptors. Effect of Ligand Functionalization on the Ability to Host Counteranions by Hydrogen Bonds

M. Isabel Ortiz,[†] M. Laura Soriano,[‡] M. Pilar Carranza,[†] Félix A. Jalón,[†] Jonathan W. Steed,[‡] Kurt Mereiter,[§] Ana M. Rodríguez,[⊥] David Quiñonero,[¶] Pere M. Deyà,[¶] and Blanca R. Manzano*[,†]

[†]*Departamento de Química Inorgánica, Orgánica y Bioquímica, Facultad de Químicas, IRICA, Universidad de Castilla—La Mancha, Avenida Camilo José Cela 10, E-13071 Ciudad Real, Spain,* [‡]*Department of Chemistry, Durham University, South Road, Durham DH1 3LE, U.K.,* [§]*Faculty of Chemistry, Vienna University of Technology, Getreidemarkt 9/164SC, A-1060 Vienna, Austria,* [⊥]*Departamento de Química Inorgánica, Orgánica y Bioquímica, Escuela Técnica Superior de Ingenieros Industriales, Universidad de Castilla—La Mancha, Avenida Camilo José Cela 3, E-13071 Ciudad Real, Spain, and* [¶]*Departament de Química, Universitat de les Illes Balears, Crta. Valldemossa km 7.5, 07122 Palma de Mallorca, Spain*

Received May 18, 2010

Several complexes with a [2 × 2] grid structure have been obtained by the self-assembly of different copper(I) salts and ligands of the type 4,6-bis(pyrazol-1-yl)pyrimidine containing different substituents on the heterocycles. The main goal has been to evaluate the influence over the solid state and solution behavior of the functionalization of the pyrimidine ring with a primary amino substituent. The molecular and crystalline structures of some derivatives have been determined by X-ray diffraction. The grids contain two open voids formed by pairs of ligands facing one another on opposite sides of the grid in a somewhat divergent manner. One counteranion is hosted in each void interacting through hydrogen bonds and anion−π interactions. The presence of the amino group that points toward the inside of the cavity dominates the interactions in the void and apparently determines the orientation of the hosted counteranion and that of the ligands. With the exception of the derivative with chloride as the anion, the grid structure is preserved in solution (NMR and UV−vis) and some cation−anion interaction, increased by the presence of the amino group, exists also in solution (DOSY experiments). The experiments of anion interchange performed in solution indicate that a higher stability is found for the host−guest aggregates with OTs^- (*p*-Me-$C_6H_4SO_3$) and NO_3^-. While for these anions a 1:2 stoichiometry is reached, for the rest of the anions tested (ReO_4^-, OTf^-, and PF_6^-), only weaker 1:1 complexes are formed. Computational studies support the presence of anion−π interactions.

Introduction

The concept of a receptor, inspired in Nature, that was initially introduced by Paul Ehrlich and the revolutionary ideas of Alfred Werner on coordination chemistry laid the foundations of the nowadays known as host−guest chemistry.[1] Within this field, the supramolecular chemistry of anions, although less explored than that of cations, is receiving increasing attention.[2] The possible applications of anion hosts are mainly related to anion sensing,[3] transport,[4] or supramolecular catalysis.[5] During the past few years, there has been extensive work devoted to the identification of new host types.[6] Most of these systems are organic cationic or neutral hosts that are functionalized with amino, amido, and, less commonly, OH groups.[7] Besides, the importance of the C−H···anion interactions in anion−host systems has

*To whom correspondence should be addressed. E-mail: Blanca.Manzano@uclm.es. Fax: (int.) + 34-926295318.

(1) (a) *Encyclopedia of Supramolecular Chemistry*; Atwood, J. L., Steed, J. W., Eds.; Marcel Dekker, Inc.: New York, 2004. (b) *Supramolecular Chemistry*; Atwood, J. L., Steed, J. W., Eds.; John Wiley and Sons Inc.: London, 2009. (c) Hof, F.; Craig, S. L.; Nuckolls, C.; Rebek, J., Jr. *Angew. Chem., Int. Ed.* **2002**, *41*, 1488–1508.

(2) (a) *Supramolecular Chemistry of Anions*; Bianchi, A., Bowman-James, K., García-España, E., Eds.; Wiley-VCH: New York. 1997. (b) Filby, M. H.; Steed, J. W. *Coord. Chem. Rev.* **2006**, *250*, 3200–3218. (c) Gale, P. A. *Coord. Chem. Rev.* **2000**, 181–233. (d) Gale, P. A. *Coord. Chem. Rev.* **2001**, *213*, 79–128. (e) Gale, P. A.; García-Garrido, S. E.; Garric, J. *Chem. Soc. Rev.* **2008**, *37*, 151–190 and references cited therein.

(3) Lavigne, J. J.; Anslyn, E. V. *Angew. Chem., Int. Ed.* **2001**, *40*, 3119–3130.

(4) (a) Gale, P. A.; Light, M. E.; McNally, B.; Navakhum, K.; Sliwinski, K. E.; Smith, B. D. *Chem. Commun.* **2005**, 3773–3775. (b) Smith, B. D.; Lambert, T. N. *Chem. Commun.* **2003**, 2261–2268.

(5) (a) Chae, M. K.; Suk, J.-M.; Jeong, K.-S. *Tetrahedron Lett.* **2010**, *51*, 4240–4242. (b) De, Ch. K.; Klauber, E. G.; Seidel, D. *J. Am. Chem. Soc.* **2009**, *131*, 17060–17061. (c) Martinez-Garcia, H.; Morales, D.; Perez, J.; Coady, D. J.; Bielawski, Ch. W.; Gross, D. E.; Cuesta, L.; Marquez, M.; Sessler, J. L. *Organometallics* **2007**, *26*, 6511–6514. (d) Thomas, J.-L.; Howarth, J.; Hanlon, K.; McGuirk, D. *Tetrahedron Lett.* **2000**, *41*, 413–416. (e) Hosseini, M. W.; Blacker, A. J.; Lehn, J. M. *J. Chem. Soc., Chem. Commun.* **1988**, 596–598.

Published on Web 09/02/2010

recently been recognized.[8] Although in the early years metallic cations were used as Lewis acid centers where the anions were coordinated, the participation of metallic centers as a structural component in the host has only been explored extensively in the past few years.[9] In this context, organometallic receptors,[2a,b] cages,[10] helicates,[11] and metallacalixarenes[12] have been described, among others. It is important to consider that, in the preparation of cavitands, the coordination of ligands to metallic centers offers the advantage, with respect to conventional organic routes, of spontaneous construction by self-assembly. This construction is governed by the encoded structural information of the metallic center coordination preferences and of the geometrical disposition of the donor atoms of the ligands.[13]

Chart 1. Schematic Representation of the [2 × 2] Grids Decorated with Amino Groups inside the Cavity

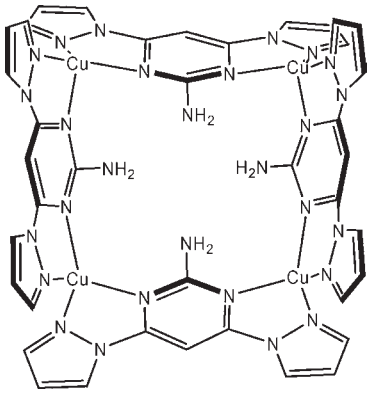

In this way, we[14] recently described the synthesis by self-assembly of a new type of [2 × 2] grid in which the facing ligands are divergent (Chart 1) and defined a new type of cavity in which the counteranions are hosted through hydrogen bonds and anion−π interactions.[8,14,15] As organic components, we used 4,6-bis(pyrazol-1-yl)pyrimidine or other similar ligands with methylated pyrazolyl rings and copper(I) as the metallic center. These assemblies exhibit some conformational flexibility. This new type of grid can be considered as cavitands, reminiscent of those described by Cram et al. on the basis of oligomeric dibenzofurans of a cyclic structure.[16]

Anion hosts may be classified as rigid or flexible. If the host does not undergo a significant conformational change upon guest binding, it is considered as preorganized and usually the free energy of complexation is more favorable. However, a high rigidity may lead to high activation barriers and slow kinetics. On the contrary, flexible hosts, although less favorable from an energetic point of view, may offer the advantage of fast response times and reversible binding. The present grid systems may be considered to have intermediate flexibility. The voids have a specific shape, but the angles and orientations of the ligands may vary to a certain extent. Thus, we decided to explore the anion encapsulation properties of these types of grids. The cationic charge will favor the interaction with the anions, and we decided to include in the ligand a group, NH_2, to enhance the formation of hydrogen bonds with the encapsulated anions. The acidity of this group is likely to be enhanced by the π acidity of the pyrimidine ring. Considering that the substituents in position 2 of the pyrimidine ring are oriented toward the inside of the cavity as the grid is formed (see Chart 1), we have functionalized this heterocycle with the amino group in this position. With this design, the target grids will be decorated with four NH_2

(6) (a) Caltagirone, C.; Gale, Ph. A. *Chem. Soc. Rev.* **2009**, *38*, 520–563. (b) Morakot, N.; Rakrai, W.; Keawwangchai, S.; Kaewtong, Ch.; Wanno, B. *J. Mol. Model.* **2010**, *16*, 129–136. (c) Sahin, O.; Memon, Sh.; Yilmaz, M. *J. Macromol. Sci. A* **2010**, *47*, 20–25. (d) Edwards, P. R.; Hiscock, J. R.; Gale, P. A.; Light, M. E. *Org. Biomol. Chem.* **2010**, *8*, 100–106. (e) Hermida-Ramón, J. M.; Mandado, M.; Sánchez-Lozano, M.; Estévez, C. M. *Phys. Chem. Chem. Phys.* **2010**, *12*, 164–169.

(7) (a) Amendola, V.; Fabrizzi, L. *Chem. Commun.* **2009**, 513–531. (b) Steed, J. W. *Chem. Soc. Rev.* **2009**, *38*, 506–519. (c) Rice, C. R. *Coord. Chem. Rev.* **2006**, *250*, 3190–3199. (d) Chmielewski, M. J.; Zielinski, T.; Jurczak, J. *Pure Appl. Chem.* **2007**, *79*, 1087–1096.

(8) (a) Bryantsev, V. S.; Hay, B. P. *J. Am. Chem. Soc.* **2005**, *127*, 8282–8283. (b) Turner, D. R.; Paterson, M. J.; Steed, J. W. *J. Org. Chem.* **2006**, *71*, 1598–1608. (c) Li, Y.; Flood, A. H. *Angew. Chem., Int. Ed.* **2008**, *47*, 2649–2652. (d) Zhu, S. S.; Staats, H.; Brandhorst, K.; Grunenberg, J.; Gruppi, F.; Dalcanale, E.; Lützen, A.; Rissanen, K.; Schalley, C. A. *Angew. Chem., Int. Ed.* **2008**, *47*, 788–792. (e) Li, Y.; Flood, A. H. *J. Am. Chem. Soc.* **2008**, *130*, 12111–12122. (f) Hay, B. P.; Bryantsev, V. S. *Chem. Commun.* **2008**, 2417–2428. (g) Yoon, D.-W.; Gross, D. E.; Lynch, V. M.; Sessler, J. L.; Hay, B. P.; Lee, C.-H. *Angew. Chem., Int. Ed.* **2008**, *47*, 5038–5942. (h) Pedizisa, L.; Hay, B. P. *J. Org. Chem.* **2009**, *74*, 2554–2560.

(9) (a) Fujita, M. *Chem. Soc. Rev.* **1998**, *27*, 417–425. (b) Yoshizawa, M.; Tamura, M.; Fujita, M. *Science* **2006**, *312*, 251–254. (c) Fiedler, D.; van Halbeek, H.; Bergman, R. G.; Raymond, K. N. *J. Am. Chem. Soc.* **2006**, *128*, 10249–10252. (d) Steed, J. W. *Chem. Soc. Rev.* **2009**, *38*, 506–518.

(10) (a) Vilar, R.; Mingos, D. M. P.; White, A. J. P.; Williams, D. J. *Angew. Chem., Int. Ed.* **1998**, *37*, 1258–1261. (b) Fleming, J. S.; Mann, K. L. V.; Carraz, C.-A.; Psillakis, E.; Jeffery, J. C.; McCleverty, J. A.; Ward, M. D. *Angew. Chem., Int. Ed.* **1998**, *37*, 1279–1281. (c) Paul, R. L.; Bell, Z. R.; Fleming, J. S.; Jeffery, J. C.; McCleverty, J. A.; Ward, M. D. *Heteroatom. Chem.* **2002**, *13*, 567–573. (d) Su, C.-Y.; Cai, Y.-P.; Chen, C.-L.; Lissner, F.; Kang, B.-S.; Kaim, W. *Angew. Chem., Int. Ed.* **2002**, *41*, 3371–3375. (e) Amouri, H.; Desmarets, C.; Bettoschi, A.; Rager, M. N.; Boubekeur, K.; Rabu, P.; Drillon, M. *Chem.—Eur. J.* **2007**, *13*, 5401–5407.

(11) (a) McMorran, D. A.; Steel, P. J. *Angew. Chem., Int. Ed.* **1998**, *37*, 3295–3297. (b) Hasenknopf, B.; Lehn, J.-M.; Kneisel, B. O.; Baum, G.; Fenske, D. *Angew. Chem., Int. Ed. Engl.* **1996**, *35*, 1838–1840.

(12) (a) Navarro, J. A. R.; Janik, M. B. L.; Freisinger, E.; Lippert, B. *Inorg. Chem.* **1999**, *38*, 426–432. (b) Barea, E.; Navarro, J. A. R.; Salas, J. M.; Quirós, M.; Willermann, M.; Lippert, B. *Chem.—Eur. J.* **2003**, *9*, 4414–4421. (c) Galindo, M. A.; Navarro, J. A. R.; Romero, M. A.; Quirós, M. *Dalton Trans.* **2004**, 1563–1566.

(13) (a) Lehn, J.-M. *Supramolecular Chemistry—Cconcepts and Perspectives*; VCH: Weinheim, Germany, 1995. (b) Baxter, P. N. M. In *Comprehensive Supramolecular Chemistry*; Atwood, J. L., Davies, J. E. D., MacNicol, D. D., Vögtle, F., Lehn, J.-M., Eds.; Pergamon Press: Oxford, U.K.; Vol. *9*, 1996; pp 165−211. (c) Constable, E. C. in the same reference, pp 213−252. (d) Fujita, M. in the same reference, pp 253−282.

(14) Manzano, B. R.; Jalón, F. A.; Ortiz, I. M.; Soriano, M. L.; Gómez de la Torre, F.; Elguero, J.; Maestro, M. A.; Mereiter, K.; Claridge, T. D. V. *Inorg. Chem.* **2008**, *47*, 413–428.

(15) (a) Schottel, B. L.; Chifotides, H. T.; Dunbar, K. R. *Chem. Soc. Rev.* **2008**, *37*, 68–83. (b) Mascal, M.; Armstrong, A.; Bartberger, M. *J. Am. Chem. Soc.* **2002**, *124*, 6274–6276. (c) Alkorta, I.; Rozas, I.; Elguero, J. *J. Am. Chem. Soc.* **2002**, *124*, 8593–8598. (d) Quiñonero, D.; Garau, C.; Rotger, C.; Frontera, A.; Ballester, P.; Costa, A.; Deyà, P. M. *Angew. Chem., Int. Ed.* **2002**, *41*, 3389–3392. (e) Berryman, O. B.; Bryantsev, V. S.; Stay, D. P.; Johnson, D. W.; Hay, B. P. *J. Am. Chem. Soc.* **2007**, *129*, 48–58. (f) Demeshko, S.; Dechert, S.; Meyer, F. *J. Am. Chem. Soc.* **2004**, *126*, 4508–4509. (g) Schottel, B. L.; Bacsa, J.; Dunbar, K. R. *Chem. Commun.* **2005**, 46–47. (h) de Hoog, P.; Gamez, P.; Mutikainen, I.; Turpeinen, U.; Reedijk, J. *Angew. Chem., Int. Ed.* **2004**, *43*, 5815–5817. (i) Frontera, A.; Saczewski, F.; Gdaniec, M.; Dziemidowicz-Borys, E.; Kurland, A.; Deyà, P. M.; Quiñonero, D.; Garau, C. *Chem.—Eur. J.* **2005**, *11*, 6560–6567. (j) Barrios, L. A.; Aromi, G.; Frontera, A.; Quiñonero, D.; Deyà, P. M.; Gamez, P.; Roubeau, O.; Shotton, E. J.; Teat, S. J. *Inorg. Chem.* **2008**, *47*, 5873–5881. (k) Mascal, M. *Angew. Chem., Int. Ed.* **2006**, *45*, 2890–2893. (l) Mooibroek, T. J.; Black, C. A.; Gamez, P.; Reedijk, J. *Cryst. Growth. Des.* **2008**, *8*, 1082–1093. (m) Gamez, P.; Mooibroek, T. J.; Teat, S. J.; Reedijk, J. *Acc. Chem. Res.* **2007**, *40*, 435–444. (n) Staffilani, M.; Hancock, K. S. B.; Steed, J. W.; Holman, K. T.; Atwood, J. L.; Juneja, R. K.; Burkhalter, R. S. *J. Am. Chem. Soc.* **1997**, *119*, 6324–6335. (o) Carranza, M. P.; Manzano, B. R.; Jalón, F. A.; Rodríguez, A. M.; Santos, L.; Moreno, M. *Inorg. Chem.* **2010**, *49*, 3828–3835.

(16) Helgeson, R. C.; Lauer, M.; Cram, D. J. *J. Chem. Soc., Chem. Commun.* **1983**, 101–103.

groups in the core of the open voids, in such a way that the hydrogen bonds should govern the strength and disposition of the interactions with the hosted anion. Although grids where anions[17] or molecules[18] are hosted in their cavities have been previously described, the predesigned introduction of functionalities in the cavities to enhance the formation of hydrogen bonds with the anions has not been explored. Ligands containing aminopyrimidine groups have been explored in supramolecular chemistry,[19] but the goal has not been anion encapsulation.

In this work, we describe the synthesis of a set of [2 × 2] copper(I) grids functionalized with amino groups differing in the accompanying counteranion, PF_6^-, BF_4^-, ClO_4^-, *p*-Me-$C_6H_4SO_3^-$ (OTs^-), or $CF_3SO_3^-$ (OTf^-). For the sake of comparison, other nonaminated grids have also been obtained. The main goal is, as stated, the study of the influence of the amino group in the ligand over the anion encapsulation properties. More specifically, we will study the effect of this group over (i) the strength of the anion interactions with the walls of the cavities, (ii) the orientation adopted by the encapsulated anions in the solid state, (iii) the stability of the grids in solution and its ability to retain the anion making a comparison between the different anions, and (iv) the possibility and selectivity of anion interchange both in the solid state and in solution.

Experimental Section

General Comments. All of the manipulations were carried out under an atmosphere of dry oxygen-free nitrogen using standard Schlenk techniques. Solvents were distilled from appropriate drying agents and degassed before use. Elemental analyses were performed with a Thermo Quest Flash EA 1112 microanalyzer. IR spectra were recorded as KBr pellets or Nujol mulls with a Jasco FTIR-6300 type A spectrometer or in a Shimadzu IR-PRESTIGE-21 spectrometer equipped with an attenuated total reflectance (ATR) device. UV−vis spectra were recorded in a Jasco UV−vis V-530 spectrophotometer. Positive-mode fast-atom-bombardment mass spectrometry (FAB^+ MS) measurements were made with a VG BIOTECH QUATTRO spectrometer. Powder X-ray diffraction patterns were recorded with a Bruker D8 Advance system with Cu Kα radiation. ^1H, $^{13}C\{^1H\}$, ^{19}F, and $^{31}P\{^1H\}$ NMR spectra were recorded on a Varian Unity FT-300, a Varian Gemini FT-400, or an Innova TF-500 spectrometer. Chemical shifts (ppm) are relative to tetramethylsilane (TMS; ^1H and ^{13}C NMR), $CFCl_3$ (^{19}F NMR), or 85% H_3PO_4 (^{31}P NMR). Use Chart 2 for numbering. Coupling constants (*J*) are in Hertz. The NOE difference spectra were recorded with a 5000 Hz spectrum width, acquisition time 3.27 s, pulse width 90°, relaxation delay 4 s, irradiation power 5−10 dB, and number of scans 240. For $^1H-^{13}C$, g-HSQC, and g-HMBC NMR spectra, the standard Varian pulse sequences were used (*VNMR 6.1 C* software). The spectra were acquired using 7996 (^1H) and 25133.5 (^{13}C) Hz spectral widths; 16 transients of 2048 data points were collected for each of the 256 increments. For low-temperature spectra, the probe temperature (1 K) was controlled by a standard unit calibrated with a methanol reference. In the NMR data, s, d, t, and b refer to singlet, doublet, triplet, and broad, respectively. The carbon resonances are singlets. Resonances marked with double prime belong to the *p*-$CH_3C_6H_4SO_3$ counteranion. Diffusion NMR measurements were carried out with a Bruker DRX500 using the BPP-LED sequence,[20] with sample temperatures regulated at 298 K. A Bruker triple-resonance inverse probe head was employed on which the nominal ^1H channel could also be turned down to ^{19}F, allowing measurements on both nuclei. Sample spinning at 20 Hz was employed to eliminate convection interference[21] with diffusion periods (Δ = 50 ms) selected to ensure integer tube revolutions during this time. Diffusion encoding gradients were set to 4 ms total duration (δ) and were applied as bipolar pairs,[22] with typically 8−16 gradient increments employed to map the diffusion behavior. Data were analyzed with either the curve-fitting routines provided in Bruker's *XWINNMR* software or with fitting routines within suitable Microsoft Excel spreadsheets using the Solver tool. Pyrazole, 3,5-dimethylpyrazole, 2-amino-4,6-dichloropyrimidine, 2-methyl-4,6-dichloropyrimidine, and AgOTf were purchased from Aldrich. $[Cu(CH_3CN)_4]X$ (X = PF_6, BF_4, ClO_4, and OTs)[23] and CuCl[24] salts were prepared according to the literature procedures.

Chart 2

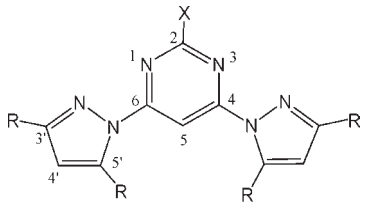

X = NH_2; R = H; bpzapm
X = NH_2; R = Me; bpz*apm
X = Me; R = H; bpzmpm
X = Me; R = Me; bpz*mpm

X-ray Structure Determination. Orange crystals of compounds **3**, **6**, and **7** in the form of solvates were obtained by diffusion of the starting reagents in mixture of the following phases: $[Cu(CH_3CN)_4]X$ salt in dichloromethane/acetone/ligand in dibutyl ether. This procedure furnished in the cases of **6** and **7** coexisting solvate polymorphs of tetragonal, monoclinic, and triclinic symmetry, of which only the most stable triclinic ones were subjected to further investigations reported here. Red crystals of **17**, also as a solvate, were obtained by the slow evaporation of an acetone solution of the complex. Orange crystals of **18**·4acetone were obtained by the slow diffusion of pentane into a solution of the complex in acetone.

X-ray data of **3**·solv, **6**·solv, **7**·solv, **17**·solv, and **18**·4acetone were collected with Bruker Smart/Kappa APEX CCD diffractometers at *T* = 150−173 K using graphite-monochromated Mo Kα radiation (λ = 0.710 73 Å, sealed X-ray tubes) and 0.3° ω-scan frames covering complete spheres of the reciprocal space up to θ_{max} = 25° or 28.3°. After data integration with the program *SAINT*, corrections for absorption, λ/2 effects, and crystal decay were applied with the program

(17) (a) Ruben, M.; Rojo, J.; Romero-Salguero, F. J.; Uppadine, L. H.; Lehn, J.-M. *Angew. Chem., Int. Ed.* **2004**, *43*, 3644–3662. (b) Campos-Fernández, C. S.; Clérac, R.; Dunbar, K. R. *Angew. Chem., Int. Ed.* **1999**, *38*, 3477–3479. (c) Cati, D. S.; Ribas, J.; Ribas-Ariño, J.; Stoeckli-Evans, H. *Inorg. Chem.* **2004**, *43*, 1021–1030. (d) Patroniak, V.; Baxter, P. N. W.; Lehn, J.-M.; Kubicki, M.; Nissinen, M.; Rissanen, K. *Eur. J. Inorg. Chem.* **2003**, *42*, 4001–4009.

(18) (a) Toyota, S.; Woods, C. R.; Benaglia, M.; Haldimann, R.; Wärnmark, K.; Hardcastle, K.; Siegel, J. S. *Angew. Chem., Int. Ed.* **2001**, *40*, 751–754. (b) Baxter, P. N. W.; Lehn, J.-M.; Kneisel, B. O.; Fenske, D. *Chem. Commun.* **1997**, 2231–2232.

(19) (a) Ziener, U.; Breuning, E.; Lehn, J.-M.; Wegelius, E.; Rissanen, K.; Baum, G.; Fenske, D.; Vaughan, G. *Chem.—Eur. J.* **2000**, *6*, 4132–4139. (b) Luo, G.-G.; Huang, R.-B.; Chen, J.-H.; Lin, L.-R.; Zheng, L.-S. *Polyhedron* **2008**, *27*, 2791–2798. (c) Luo, G.-G.; Huang, R.-B.; Zhang, N.; Lin, L.-R.; Zheng, L.-S. *Polyhedron* **2008**, *27*, 3231–3238.

(20) Wu, D.; Chen, A.; Johnson, C. S. *J. Magn. Reson., Ser. A* **1995**, *115*, 260–264.

(21) Esturau, N.; Sánchez-Ferrando, F.; Gavin, J. A.; Roumestand, C.; Delsuc, M.-A.; Parella, T. *J. Magn. Reson.* **2001**, *153*, 48–55.

(22) Wider, G.; Dötsch, V.; Wüthrich, K. *J. Magn. Reson., Ser. A* **1994**, *108*, 255–258.

(23) Kubas, G. J. *Inorg. Synth.* **1979**, *19*, 90–92.

(24) Keller, R. N.; Wycoff, H. D. *Inorg. Synth.* **1962**, *2*, 1–4.

Table 1. Crystal Data and Structure Refinement for Complexes **3**, **6**, **7**, **17**, and **18**

	3·solv[a]	**6**·solv[a]	**7**·solv[a]	**17**·solv[a]	**18**·4acetone
empirical formula	$C_{40}H_{36}Cl_4Cu_4N_{28}O_{16}$	$C_{56}H_{68}B_4Cu_4F_{16}N_{28}$	$C_{56}H_{68}Cl_4Cu_4N_{28}O_{16}$	$C_{60}H_{68}Cu_4F_{12}N_{28}O_{12}S_4$	$C_{76}H_{96}Cu_4F_{12}N_{24}O_{16}S_4$
fw	1560.93	1734.78	1785.34	1983.90	2212.25
T (K)	173	173	173	173	150
cryst size (mm^3)	0.50 × 0.38 × 0.28	0.72 × 0.22 × 0.21	0.40 × 0.15 × 0.12	0.66 × 0.58 × 0.34	0.31 × 0.30 × 0.11
cryst syst	monoclinic	triclinic	triclinic	monoclinic	orthorhombic
space group	$C2/m$ (No. 12)	$P\bar{1}$ (No. 2)	$P\bar{1}$ (No. 2)	$C2/m$ (No. 12)	$Fdd2$ (No. 43)
Z	4	2	2	4	8
a (Å)	23.3630(13)	15.4109(8)	15.4660(6)	27.5148(16)	31.496(2)
b (Å)	15.3043(8)	15.8760(8)	15.8994(6)	26.7525(16)	39.922(2)
c (Å)	20.5706(11)	20.2866(10)	20.4336(8)	15.8348(9)	15.062(2)
α (deg)	90	94.910(1)	94.796(1)	90	90
β (deg)	111.049(1)	100.478(1)	100.840(1)	111.230(1)	90
γ (deg)	90	118.410(1)	118.353(1)	90	90
V (Å^3)	6864.3(6)	4207.0(4)	4255.2(3)	10864.8(11)	18939(3)
ρ_{calcd} (g cm^{-3})	1.510	1.369	1.393	1.213	1.552
μ_{calcd} (mm^{-1})	1.456	1.084	1.184	0.925	1.073
F(000)	3136	1760	1824	4032	9088
θ_{max} (deg)	25.0	25.0	25.0	25.0	28.3
total reflns measd	35 071	43 584	44 530	52 469	38 742
indep reflns [R_{int}]	6288 [0.041]	14 749 [0.024]	14 925 [0.040]	9786 [0.022]	11 637 [0.092]
indep reflns [$I > 2\sigma(I)$]	4410	11959	10560	8387	7177
params refined/restraints	475/0	1079/142	1051/39	582/0	628/1
R1 [$I > 2\sigma(I)$]/(all data)[b]	0.0596/0.0857	0.0469/0.0552	0.0556/0.0779	0.0442/0.0489	0.0548/0.1086
wR2 [$I > 2\sigma(I)$]/(all data)[b]	0.1737/0.1924	0.1378/0.1445	0.1465/0.1570	0.1295/0.1329	0.1050/0.1280
GOF	1.102	1.096	1.079	1.103	0.954
diff Fourier peaks min/max, e Å^{-3}	−0.85/0.87	−0.49/0.99	−0.74/0.98	−0.62/0.69	−0.50/0.68

[a] Disordered solvent was SQUEEZED with the program *PLATON*.[26] The chemical formulas and derived quantities F_w, ρ(calc), μ_{calcd}, and F(000) are given without solvent contributions. [b] $R1 = \sum||F_o| - |F_c||/\sum|F_o|$ and $wR2 = \{\sum[w(F_o^2 - F_c^2)^2]/\sum[(w(F_o^2)^2]\}^{1/2}$.

SADABS.[25] The structures were solved with direct methods and refined by full-matrix least-squares methods based on F^2 using *SHELXTL*.[25] H atoms were placed in calculated positions and thereafter treated as riding atoms. A significant issue with the structures of **3**, **6**, **7**, and **17** was their considerable content of disordered solvent molecules (or mixtures thereof) combined with an orientation disorder of part of the anions. After elaborate attempts to include some discrete solvent molecules in the structure refinement, it was found advantageous to remove the all solvents from structure factor calculations prior to final refinement by applying the procedure *SQUEEZE* of the program *PLATON*.[26] Only the structure **18**·4acetone was well ordered in solvents and anions. Important crystallographic data are summarized in Table 1, and further details can be found in the Supporting Information in CIF format. Structural graphics were prepared with *SHELXTL* and the program *MERCURY*.[25,27]

Syntheses of the New Ligands. 2-Amino-4,6-bis(pyrazol-1-yl)-pyrimidine (bpzapm). A solution of pyrazole (1.299 g, 19.1 mmol) was added to a solution of NaH (0.458 g, 19.1 mmol) in 10 mL of tetrahydrofuran (THF; the mineral oil was previously washed with 3 × 10 mL of hexane). The reaction mixture was stirred for 2 h at room temperature. Then 0.783 g (4.40 mmol) of 2-amino-4,6-dichloropyrimidine in anhydrous THF was added to the suspension of the pyrazolate sodium salt. After 48 h at room temperature, the suspension was evaporated under vacuum. The precipitate was extracted with 3 × 30 mL of CH_2Cl_2 and then was purified by column chromatography on silica gel using hexane/ethyl acetate in a 1:5 ratio or crystallized in CH_2Cl_2/pentane. Yield: 0.560 g (2.46 mmol, 56%). Anal. Calcd for $C_{10}H_9N_7$: C, 52.86; H, 3.99; N, 43.15. Found: C, 52.64; H, 3.84; N, 43.07. ^{1}H NMR (acetone-d_6, 500 MHz, 25 °C): δ 8.54 (d, 2H, $J_{5'-4'}$ = 2.7 Hz, H$^{5'}$), 7.81 (d, 2H, $J_{3'-4'}$ = 1.2 Hz, H$^{3'}$), 7.76 (s, 1H, H^5), 6.55 (dd, 2H, H$^{4'}$), 6.54 (bs, 2H, NH_2) ppm. ^{1}H NMR ($CDCl_3$, 500 MHz, 25 °C): δ 8.40 (d, 2H, $J_{5'-4'}$ = 2.5 Hz, H$^{5'}$), 7.72 (s, 1H, H^5), 7.67 (d, 2H, $J_{3'-4'}$ = 1.2 Hz, H$^{3'}$), 6.37 (dd, 2H, H$^{4'}$), 5.36 (bs, 2H, NH_2) ppm. ^{13}C{^{1}H} NMR (acetone-d_6, 500 MHz, 25 °C): δ 163.8 (s, 1C, C^2), 160.1 (s, 2C, C^{4,6}), 143.4 (s, 2C, C$^{3'}$), 127.4 (s, 2C, C$^{5'}$), 108.5 (s, 2C, C$^{4'}$), 84.8 (s, 1C, C^5) ppm. ^{13}C{^{1}H} NMR ($CDCl_3$, 500 MHz, 25 °C): δ 162.6 (s, 1C, C^2), 160.0 (s, 2C, C^{4,6}), 143.4 (s, 2C, C$^{3'}$), 127.7 (s, 2C, C$^{5'}$), 108.6 (s, 2C, C$^{4'}$), 86.4 (s, 1C, C^5) ppm. IR (Nujol): ν/cm^{-1} 3374, 3326 [$\nu(NH_2)$], 1646, 790 [$\delta(NH_2)$], 1580 [ν(CN/CC)].

2-Amino-4,6-bis(3,5-dimethylpyrazol-1-yl)pyrimidine (bpz*apm). The procedure is similar to that of bpzapm. The amounts were as follows: 0.433 g (18.05 mmol) of NaH, 1.735 g (18.05 mmol) of 3,5-dimethylpyrazole, and 0.740 g (4.51 mmol) of 2-amino-4,6-dichloropyrimidine. The reaction took place over 48 h at the refluxing temperature of the solvent (THF). The ligand was recrystallized in dichloromethane/pentane. Yield: 0.761 g (2.68 mmol, 57%). Anal. Calcd for $C_{14}H_{17}N_7$: C, 59.35; H, 6.05; N, 34.60. Found: C, 59.20; H, 6.01; N, 34.87. ^{1}H NMR (acetone-d_6, 500 MHz, 25 °C): δ 7.73 (s, 1H, H^5), 6.31 (s, 2H, NH_2), 6.06 (s, 2H, H$^{4'}$), 2.68 (s, 6H, Me$^{5'}$), 2.22 (2, 6H, Me$^{3'}$) ppm. ^{1}H NMR (acetone-d_6, 500 MHz, −80 °C): δ 7.69 (s, 1H, H^5), 7.11 (s, 2H, NH_2), 6.15 (s, 2H, H$^{4'}$), 2.60 (s, 6H, Me$^{5'}$), 2.20 (2, 6H, Me$^{3'}$) ppm. ^{1}H NMR ($CDCl_3$, 400 MHz, 25 °C): δ 7.69 (s, 1H, H^5), 5.98 (s, 2H, H$^{4'}$), 4.99 (s, 2H, NH_2), 2.67 (s, 6H, Me$^{5'}$), 2.29 (s, 6H, Me$^{3'}$) ppm. ^{13}C{^{1}H} NMR (acetone-d_6, 500 MHz, 25 °C): δ 162.1 (s, 3C, C^{2,4,6}), 150.5 (s, 2C, C$^{3'}$), 142.7 (s, 2C, C$^{5'}$), 110.1 (s, 2C, C$^{4'}$), 88.5 (s, 1C, C^5), 15.1 (s, 2C, Me$^{5'}$), 13.0 (s, 2C, Me$^{3'}$) ppm. ^{13}C{^{1}H} NMR ($CDCl_3$, 500 MHz, 25 °C): δ 161.8 (s, 3C, C^{2,4,6}), 151.1 (s, 2C, C$^{3'}$), 142.5 (s, 2C, C$^{5'}$), 110.4 (s, 2C, C$^{4'}$), 91.3 (s, 1C, C^5), 15.5 (s, 2C, Me$^{5'}$), 14.0 (s, 2C, Me$^{3'}$) ppm. IR (Nujol): ν/cm^{-1} 3441, 3339, 3221, 3199 [$\nu(NH_2)$], 1628, 1609, 794 [δ-(NH_2)], 1583 [ν(CN/CC)]. UV−vis (CH_2Cl_2): λ (ε) 223 (3.9 × 10^5), 253 (2.9 × 10^5), 307 (3.7 × 10^5) nm.

2-Methyl-4,6-bis(pyrazol-1-yl)pyrimidine (bpzmpm). The procedure is similar to that of bpzapm. The amounts were as

(25) (a) Bruker software *SAINT*, *SADABS*, and *SHELXTL*; Bruker AXS Inc.: Madison, WI, 2003−2008. (b) Sheldrick, G. M. *Acta Crystallogr.* **2008**, *A64*, 112–122.
(26) Spek, A. L. *Acta Crystallogr.* **2009**, *D65*, 148–155.
(27) Macrae, C. F.; Edgington, P. R.; McCabe, P.; Pidcock, E.; Shields, G. P.; Taylor, R.; Towler, M.; van de Streek, J. *J. Appl. Crystallogr.* **2006**, *39*, 453–457.

follows: 0.213 g (8.88 mmol) of NaH, 0.604 g (8.88 mmol) of pyrazole, and 0.724 g (4.41 mmol) of 2-methyl-4,6-dichloropyrimidine. The reaction took place over 16 h at room temperature in 30 mL of THF. From the crude product, the ligand was obtained by extraction with CH_2Cl_2 (6 × 30 mL). The ligand was recrystallized in dichloromethane/pentane. Yield: 0.622 g (2.75 mmol, 62%). Anal. Calcd for $C_{11}H_{10}N_6$: C, 58.46; H, 4.46; N, 37.15. Found: C, 58.24; H, 4.31; N, 36.94. ^{1}H NMR (acetone-d_6, 500 MHz, 25 °C): δ 8.68 (d, 2H, $J_{5'-4'}$ = 2.0 Hz, $H^{5'}$), 7.88 (bs, 2H, $H^{3'}$), 8.24 (s, 1H, H^5), 6.62 (t, 2H, $H^{4'}$), 2.68 (s, 3H, Me_{pm}) ppm. ^{1}H NMR ($CDCl_3$, 500 MHz, 25 °C): δ 8.62 (d, 2H, $J_{5'-4'}$ = 2.4 Hz, $H^{5'}$), 8.31 (s, 1H, H^5), 7.81 (bs, 2H, $H^{3'}$), 6.51 (t, 2H, $H^{4'}$), 2.62 (s, 3H, Me_{pm}) ppm. $^{13}C\{^1H\}$ NMR (acetone-d_6, 500 MHz, 25 °C): δ 168.7 (s, 1C, C^2), 159.2 (s, 2C, $C^{4,6}$), 144.1 (s, 2C, $C^{3'}$), 127.9 (s, 2C, $C^{5'}$), 109.2 (s, 2C, $C^{4'}$), 92.1 (s, 1C, C^5), 25.2 (s, 1C, Me_{pm}) ppm. $^{13}C\{^1H\}$ NMR ($CDCl_3$, 500 MHz, 25 °C): δ 168.5 (s, 1C, C^2), 159.2 (s, 2C, $C^{4,6}$), 143.9 (s, 2C, $C^{3'}$), 128.0 (s, 2C, $C^{5'}$), 108.9 (s, 2C, $C^{4'}$), 93.0 (s, 1C, C^5), 26.1 (s, 1C, Me_{pm}) ppm. IR (Nujol): ν/cm^{-1} 1565 [ν(CN/CC)].

2-Methyl-4,6-bis(3,5-dimethylpyrazol-1-yl)pyrimidine (bpz*mpm). The procedure is similar to that of bpzapm. The amounts were as follows: 0.236 g (9.82 mmol) of NaH, 0.943 g (9.82 mmol) of 3,5-dimethylpyrazole, and 0.400 g (2.45 mmol) of 2-methyl-4,6-dichloropyrimidine. The reaction took place over 16 h at the refluxing temperature of THF. From the crude product, the ligand was obtained by extraction with CH_2Cl_2 (4 × 30 mL). The ligand was recrystallized in dichloromethane/pentane. Yield: 0.442 g (1.57 mmol, 64%). Anal. Calcd for $C_{15}H_{18}N_6$: C, 63.81; H, 6.43; N, 29.76. Found: C, 63.62; H, 6.24; N, 29.52. ^{1}H NMR (acetone-d_6, 500 MHz, 25 °C): δ 8.22 (s, 1H, H^5), 6.13 (s, 2H, $H^{4'}$), 2.73 (s, 6H, $Me^{5'}$), 2.63 (s, 3H, Me_{pm}), 2.25 (2, 6H, $Me^{3'}$) ppm. ^{1}H NMR ($CDCl_3$, 500 MHz, 25 °C): δ 8.16 (s, 1H, H^5), 6.00 (s, 2H, $H^{4'}$), 2.71 (s, 6H, $Me^{5'}$), 2.65 (s, 3H, Me_{pm}), 2.30 (2, 6H, $Me^{3'}$) ppm. $^{13}C\{^1H\}$ NMR (acetone-d_6, 500 MHz, 25 °C): δ 151.8 (s, 2C, $C^{3'}$), 143.1 (s, 2C, $C^{5'}$), 111.2 (s, 2C, $C^{4'}$), 93.9 (s, 1C, C^5), 15.6 (s, 1C, Me_{pm}), 14.2 (s, 2C, $Me^{5'}$), 13.5 (s, 2C, $Me^{3'}$) ppm. $^{13}C\{^1H\}$ NMR ($CDCl_3$, 500 MHz, 25 °C): δ 166.4 (s, 1C, C^2), 161.0 (s, 2C, $C^{4,6}$), 151.5 (s, 2C, $C^{3'}$), 142.9 (s, 2C, $C^{5'}$), 110.6 (s, 2C, $C^{4'}$), 96.9 (s, 1C, C^5), 26.1 (s, 1C, Me_{pm}), 15.6 (s, 2C, $Me^{5'}$), 14.0 (s, 2C, $Me^{3'}$) ppm. IR (Nujol): ν/cm^{-1} 1591, 1563 [ν(CN/CC)].

Syntheses of the New Derivatives. [Cu(bpzapm)]$_4$(PF$_6$)$_4$ (1). A solution of 82.0 mg (0.220 mmol) of $[Cu(CH_3CN)_4]PF_6$ in 20 mL of CH_2Cl_2 was added to a solution of 50.0 mg (0.220 mmol) of bpzapm in 10 mL of CH_2Cl_2. An orange precipitate appeared instantaneously. The suspension was stirred at room temperature for 2 h, and after that, it was filtered. The obtained orange solid was washed with THF and dried under vacuum. Yield: 79.7 mg (0.183 mmol, 83%). Anal. Calcd for **1** ($C_{40}H_{36}N_{28}F_{24}P_4Cu_4$): C, 27.57; H, 2.09; N, 22.50. Found: C, 27.59; H, 2.18; N, 22.69. ^{1}H NMR (acetone-d_6, 400 MHz, 25 °C): δ 8.96 (d, 2H, $J_{5'-4'}$ = 2.9 Hz, $H^{5'}$), 8.21 (d, 2H, $J_{3'-4'}$ = 1.7 Hz, $H^{3'}$), 8.14 (s, 1H, H^5), 7.05 (dd, 2H, $H^{4'}$), 5.75 (bs, 2H, NH_2) ppm. ^{1}H NMR (acetone-d_6, 300 MHz, −80 °C): δ 8.99 (bs, 2H, $H^{5'}$), 8.29 (s, 1H, H^5), 8.26 (bs, 2H, $H^{3'}$), 7.38 (bs, 2H, NH_2), 7.14 (t, 2H, $H^{4'}$) ppm. ^{19}F NMR (acetone-d_6, 300 MHz, 25 °C): δ −72.7 (d, J_{PF} = 708.0 Hz) ppm. ^{19}F NMR (acetone-d_6, 300 MHz, −80 °C): δ −74.2 (d, J_{PF} = 708.1 Hz) ppm. $^{13}C\{^1H\}$ NMR (acetone-d_6, 500 MHz, 25 °C): δ 159.8 (s, 1C, C^2), 157.7 (s, 2C, $C^{4,6}$), 144.9 (s, 2C, $C^{3'}$), 131.3 (s, 2C, $C^{5'}$), 113.7 (s, 2C, $C^{4'}$), 85.8 (s, 1C, C^5) ppm. IR (Nujol): ν/cm^{-1} 3511, 3408 [ν(NH_2)], 1633, 792 [δ(NH_2)], 1585 [ν(CN/CC)], 842 [ν(P−F)], 558 [δ(P−F)]. MS (FAB$^+$, NBA): m/z (rel intens %): 1597 [$M^+ - PF_6$, 1.9], 1451 [$M^+ - 2PF_6$, 0.6], 1078 [M^+ − Cu − $4PF_6$, 1.2], 932 [M^+ − bpzapm − $4PF_6$, 7.2], 643 [M^+ − Cu − 2bpzapm − $4PF_6$, 42.1], 578 [M^+ − 2Cu − 2bpzapm − $4PF_6$, 44.4], 517 [M^+ − 3Cu − 2bpzapm − $4PF_6$, 23.5], 290 [M^+ − 3Cu − 3bpzapm − $4PF_6$, 100] D.

[Cu(bpzapm)]$_4$(BF$_4$)$_4$ (2). The synthesis of **2** is similar to that of **1**. The amounts of products were as follows: 69.2 mg (0.220 mmol) of $[Cu(CH_3CN)_4]BF_4$ and 50.0 mg (0.220 mmol) of bpzapm. The product was crystallized from acetone/hexane, and a microcrystalline product was obtained. Yield: 64.7 mg (0.165 mmol, 75%). Complex **2** is orange. Anal. Calcd for **2**·C_3H_6O ($C_{43}H_{42}B_4N_{28}OF_{16}Cu_4$): C, 32.93; H, 2.70; N, 25.01. Found: C, 33.10; H, 2.80; N, 24.82. ^{1}H NMR (acetone-d_6, 400 MHz, 25 °C): δ 8.98 (d, 2H, $J_{5'-4'}$ = 2.9 Hz, $H^{5'}$), 8.16 (bs, 2H, $H^{3'}$), 8.09 (s, 1H, H^5), 7.01 (dd, 2H, $H^{4'}$), 6.14 (bs, 2H, NH_2) ppm. ^{1}H NMR (acetone-d_6, 400 MHz, −80 °C): δ 8.98 (bs, 2H, $H^{5'}$), 8.25 (bs, 2H, $H^{3'}$), 8.18 (s, 1H, H^5), 7.31 (bs, 2H, NH_2), 7.12 (t, 2H, $H^{4'}$) ppm. ^{19}F NMR (acetone-d_6, 300 MHz, 25 °C): δ −153.2 (s) ppm. ^{19}F NMR (acetone-d_6, 300 MHz, −80 °C): δ −150.7 (s) ppm. $^{13}C\{^1H\}$ NMR (acetone-d_6, 500 MHz, 25 °C): δ 159.1 (s, 1C, C^2), 157.0 (s, 2C, $C^{4,6}$), 143.7 (s, 2C, $C^{3'}$), 130.4 (s, 2C, $C^{5'}$), 112.7 (s, 2C, $C^{4'}$), 84.6 (s, 1C, C^5) ppm. IR (Nujol): ν/cm^{-1} 3501, 3396 [ν(NH_2)], 1632, 791 [δ(NH_2)], 1585 [ν(CN/CC)], 1097, 1068 [ν(B−F)], 523 [δ(B−F)]. MS (FAB$^+$, NBA): m/z (rel intens %): 1423 [$M^+ - BF_4$, 0.7], 1335 [$M^+ - 2BF_4$, 0.5], 643 [M^+ − Cu − 2bpzapm − $4BF_4$, 20.7], 578 [M^+ − 2Cu − 2bpzapm − $4BF_4$, 21.3], 517 [M^+ − 3Cu − 2bpzapm − $4BF_4$, 19.8], 290 [M^+ − 3Cu − 3bpzapm − $4BF_4$, 100] D.

[Cu(bpzapm)]$_4$(ClO$_4$)$_4$ (3). The synthesis of **3** is similar to that of **1**. The amounts of products were as follows: 72.0 mg (0.220 mmol) of $[Cu(CH_3CN)_4]ClO_4$ and 50.0 mg (0.220 mmol) of bpzapm. Yield: 86.21 mg (0.204 mmol, 92%). Complex **3** is orange. Anal. Calcd for **3**·C_3H_6O·CH_2Cl_2 ($C_{44}H_{44}N_{28}O_{17}Cl_6Cu_4$): C, 31.02; H, 2.60; N, 23.02. Found: C, 30.77; H, 2.63; N, 23.00. ^{1}H NMR (acetone-d_6, 400 MHz, 25 °C): δ 8.97 (d, 2H, $J_{5'-4'}$ = 3.3 Hz, $H^{5'}$), 8.16 (bs, 2H, $J_{3'-4'}$ = 1.8 Hz, $H^{3'}$), 8.11 (s, 1H, H^5), 7.02 (dd, 2H, $H^{4'}$), 6.08 (bs, 2H, NH_2) ppm. $^{13}C\{^1H\}$ NMR (acetone-d_6, 500 MHz, 25 °C): δ 159.0 (s, 1C, C^2), 157.0 (s, 2C, $C^{4,6}$), 143.8 (s, 2C, $C^{3'}$), 130.4 (s, 2C, $C^{5'}$), 112.7 (s, 2C, $C^{4'}$), 84.9 (s, 1C, C^5) ppm. IR (Nujol): ν/cm^{-1} 3484, 3379 [ν(NH_2)], 1626, 792 [δ(NH_2)], 1585 [ν(CN/CC)], 1100, 1056 [ν(Cl−O)], 624 [δ(Cl−O)]. MS (FAB$^+$, NBA): m/z (rel intens %): 1358 [$M^+ - 2ClO_4$, 0.5], 909 [M^+ − 2Cu − bpzapm − $4ClO_4$, 6.0], 580 [M^+ − 2Cu − 2bpzapm − $4ClO_4$, 15.5], 517 [M^+ − 3Cu − 2bpzapm − $4ClO_4$, 28.8], 290 [M^+ − 3Cu − 3bpzapm − $4ClO_4$, 100] D.

[Cu(bpzapm)]$_4$(OTs)$_4$ (4). The synthesis of complex **4** is similar to that of complex **1**. The amounts of products were as follows: 79.8 mg (0.20 mmol) of $[Cu(CH_3CN)_4]OTs$ and 45.8 mg (0.20 mmol) of bpzapm. Yield: 59.5 mg (0.118 mmol, 59%). Complex **4** is orange. Anal. Calcd for **4**·$2CH_2Cl_2$ ($C_{70}H_{68}N_{28}O_{12}S_4Cl_4Cu_4$): C, 41.67; H, 3.40; N, 19.44; S, 6.36. Found: C, 41.89; H, 3.59; N, 19.15; S, 6.29. IR (Nujol): ν/cm^{-1} 3450, 3304 [ν(NH_2)], 1629, 793 [δ(NH_2)], 1585 [ν(CN/CC)], 1188 [ν(S−O)], 1033, 1010, 814, 682, 567. MS (FAB$^+$, NBA): m/z (rel intens %): 1049 [M^+ − 2OTs, 0.6], 645 [M^+ − Cu − 2bpzapm − 4OTs, 6.3], 580 [M^+ − 2Cu − 2bpzapm − 4OTs, 15.5], 524 [M^+ − 2Cu − 3bpzapm − 3OTs, 38.4], 517 [M^+ − 3Cu − 2bpzapm − 4OTs, 25.7], 290 [M^+ − 3Cu − 3bpzapm − 4OTs, 100] D.

[Cu(bpz*apm)]$_4$(PF$_6$)$_4$ (5). A solution of 65.6 mg (0.176 mmol) of $[Cu(CH_3CN)_4](PF_6)$ in 20 mL of CH_2Cl_2 was added to a solution of 50.0 mg (0.176 mmol) of bpz*apm in 10 mL of CH_2Cl_2. An orange suspension was formed that was stirred at room temperature for 2 h, concentrated, washed with 5 mL of THF, and filtered. The orange solid obtained was dried under vacuum. Yield: 85.57 mg (0.160 mmol, 91%). Anal. Calcd for **5**·$2CH_2Cl_2$ ($C_{58}H_{72}N_{28}F_{24}P_4Cl_4Cu_4$): C, 32.60; H, 3.40; N, 18.35. Found: C, 32.33; H, 3.52; N, 18.57. ^{1}H NMR (acetone-d_6, 400 MHz, 25 °C): δ 7.47 (s, 1H, H^5), 6.62 (s, 2H, $H^{4'}$), 5.39 (s, 2H, NH_2), 2.87 (s, 6H, $Me^{5'}$), 2.26 (2, 6H, $Me^{3'}$) ppm. ^{1}H NMR (acetone-d_6, 300 MHz, −80 °C): δ 7.56 (s, 1H, H^5), 7.43 (s, 2H, NH_2), 6.67 (s, 2H, $H^{4'}$), 2.93 (s, 6H, $Me^{5'}$), n (s, 6H, $Me^{3'}$) ppm. ^{19}F NMR (acetone-d_6, 300 MHz, 25 °C): δ −72.7 (d, J = 708.0 Hz) ppm. ^{19}F NMR (acetone-d_6, 300 MHz, −80 °C): δ −74.3 (d, J = 708.1 Hz) ppm. $^{13}C\{^1H\}$ NMR (acetone-d_6, 500 MHz, 25 °C): δ 158.8 (s, 1C, C^2), 157.0 (s, 2C, $C^{4,6}$), 152.0 (s, 2C, $C^{3'}$), 144.5 (s, 2C, $C^{5'}$), 114.0 (s, 2C, $C^{4'}$), 85.8 (s, 1C, C^5), 14.5 (s, 2C, $Me^{5'}$), 14.0 (s, 2C, $Me^{3'}$) ppm. IR (Nujol): ν/cm^{-1} 3499, 3396 [ν(NH_2)], 1628, 788

[δ(NH_2)], 1588 [ν(CN/CC)], 847 [ν(P−F)], 558 [δ(P−F)]. UV−vis (CH_2Cl_2): λ (ε) 261 (8.2×10^4), 299 (5.6×10^4), 325 (6.8×10^4), 396 (2.5×10^4) nm. MS (FAB$^+$, NBA): *m*/*z* (rel intens %): 1675 [$M^+ - PF_6$, 1.5], 1100 [M^+ − bpz*apm − $4PF_6$, 4.2], 755 [M^+ − Cu − 2bpz*apm − $4PF_6$, 28.5], 692 [M^+ − 2Cu − 2bpz*apm − $4PF_6$, 17.8], 629 [M^+ − 3Cu − 2bpz*apm − $4PF_6$, 85.3], 346 [M^+ − 3Cu − 3bpz*apm − $4PF_6$, 100] D.

[Cu(bpz*apm)]$_4$(BF_4)$_4$ (6). The synthesis of complex **6** is similar to that of **5**. The amounts were as follows: 55.4 mg (0.176 mmol) of [$Cu(CH_3CN)_4$](BF_4) and 50.0 mg (0.176 mmol) of the ligand bpz*apm. Complex **6** is orange. Yield: 69.3 mg (0.139 mmol, 79%). Anal. Calcd for **6** ($C_{56}H_{68}B_4N_{28}F_{16}Cu_4$): C, 38.77; H, 3.95; N, 22.61. Found: C, 38.53; H, 3.75; N, 22.34. ^{1}H NMR (acetone-d_6, 400 MHz, 25 °C): δ 7.45 (s, 1H, H^5), 6.60 (s, 2H, $H^{4'}$), 5.71 (s, 2H, NH_2), 2.88 (s, 6H, $Me^{5'}$), 2.27 (s, 6H, $Me^{3'}$) ppm. ^{1}H NMR (acetone-d_6, 300 MHz, −80 °C): δ 7.56 (s, 1H, H^5), 7.40 (s, 2H, NH_2), 6.68 (s, 2H, $H^{4'}$), 2.94 (s, 6H, $Me^{5'}$) ppm (signals of $Me^{3'}$ overlapped with that of the solvent). ^{19}F NMR (acetone-d_6, 300 MHz, 25 °C): δ −155.3 (s) ppm. ^{19}F NMR (acetone-d_6, 300 MHz, −80 °C): δ −151.6 (s) ppm. ^{13}C{^{1}H} NMR (acetone-d_6, 500 MHz, 25 °C): δ 158.9 (s, 1C, C^2), 157.0 (s, 2C, $C^{4,6}$), 151.6 (s, 2C, $C^{3'}$), 144.3 (s, 2C, $C^{5'}$), 113.8 (s, 2C, $C^{4'}$), 86.9 (s, 1C, C^5), 14.5 (s, 2C, $Me^{5'}$), 13.8 (s, 2C, $Me^{3'}$) ppm. IR (Nujol): ν/cm^{-1} 3488, 3382 [ν(NH_2)], 1627, 790 [δ(NH_2)], 1586 [ν(CN/CC)], 1063 [ν(B−F)], 521 [δ(B−F)]. UV−vis (CH_2Cl_2): λ (ε) 262 (8.4×10^4), 300 (6.2×10^4), 326 (6.8×10^4), 396 (2.6×10^4) nm. MS (FAB$^+$, NBA): *m*/*z* (rel intens %): 1647 [M^+ − BF_4, 2.6], 1558 [M^+ − $2BF_4$, 1.7], 755 [M^+ − Cu − 2bpz*apm − $4BF_4$, 28.5], 692 [M^+ − 2Cu − 2bpz*apm − $4BF_4$, 41.7], 629 [M^+ − 3Cu − 2bpz*apm − $4BF_4$, 22.2], 346 [M^+ − 3Cu − 3bpz*apm − $4BF_4$, 100] D.

[Cu(bpz*apm)]$_4$(ClO_4)$_4$ (7). The synthesis is similar to that used for complex **5**. The amounts were as follows: 57.6 mg (0.176 mmol) of [$Cu(CH_3CN)_4$]ClO_4 and 50.0 mg (0.176 mmol) of the ligand bpz*apm. Yield: 73.8 mg (0.165 mmol, 94%). Complex **7** is orange. Anal. Calcd for **7** ($C_{56}H_{68}N_{28}O_{16}Cl_4Cu_4$): C, 37.68; H, 3.84; N, 21.97. Found: C, 37.76; H, 3.55; N, 22.13. ^{1}H NMR (acetone-d_6, 400 MHz, 25 °C): δ 7.48 (s, 1H, H^5), 6.62 (s, 2H, $H^{4'}$), 5.73 (s, 2H, NH_2), 2.90 (s, 6H, $Me^{5'}$), 2.25 (s, 6H, $Me^{3'}$) ppm. ^{13}C{^{1}H} NMR (acetone-d_6, 500 MHz, 25 °C): δ 158.8 (s, 1C, C^2), 157.0 (s, 2C, $C^{4,6}$), 151.6 (s, 2C, $C^{3'}$), 144.4 (s, 2C, $C^{5'}$), 113.8 (s, 2C, $C^{4'}$), 87.1 (s, 1C, C^5), 14.6 (s, 2C, $Me^{5'}$), 13.9 (s, 2C, $Me^{3'}$) ppm. IR (Nujol): ν/cm^{-1} 3478, 3375 [ν(NH_2)], 1620, 787 [δ(NH_2)], 1587 [ν(CN/CC)], 1094 [ν(Cl−O)], 623 [δ(Cl−O)]. UV−vis (CH_2Cl_2): λ (ε) 262 (7.6×10^4), 301 (5.4×10^4), 324 (6.1×10^4), 397 (2.3×10^4) nm. MS (FAB$^+$, NBA): *m*/*z* (rel intens %): 1686 [M^+ − ClO_4, 0.4], 1588 [M^+ − $2ClO_4$, 0.2], 955 [M^+ − Cu − 2bpz*apm − $2ClO_4$, 1.7], 692 [M^+ − 2Cu − 2bpz*apm − $4ClO_4$, 13.8], 629 [M^+ − 3Cu − 2bpz*apm − $4ClO_4$, 15.6], 346 [M^+ − 3Cu − 3bpz*apm − $4ClO_4$, 100] D.

[Cu(bpz*apm)]$_4$(OTs)$_4$ (8). The synthesis of **8** is similar to that of **5**. The amounts were as follows: 70.2 mg (0.176 mmol) of [$Cu(CH_3CN)_4$](OTs) and 50.0 mg (0.176 mmol) of the ligand bpz*apm. Yield: 75.9 mg (0.141 mmol, 80%). Complex **8** is brown. Anal. Calcd for **8**·CH_2Cl_2 ($C_{85}H_{98}N_{28}O_{12}S_4Cl_2Cu_4$): C, 47.33; H, 4.58; N, 18.18; S, 5.95. Found: C, 47.41; H, 4.77; N, 17.97; S, 5.76. ^{1}H NMR (acetone-d_6, 400 MHz, 25 °C): δ 7.61 (bs, 4H, $H^{o'',m''}$), 7.24 (s, 1H, H^5), 6.57 (s, 2H, $H^{4'}$), 6.38 (s, 2H, NH_2), 2.74 (s, 6H, $Me^{5'}$), 2.22 (s, 6H, $Me^{3'}$) ppm. ^{1}H NMR (acetone-d_6, 300 MHz, −80 °C): δ 7.41 (s, 1H, H^5), 6.62 (s, 2H, $H^{4'}$), 6.52 (s, 2H, NH_2), 2.88 (s, 6H, $Me^{5'}$), ppm (signals of $Me^{3'}$ overlapped with that of the solvent). The signals of the anion are not observed probably because they are broad. ^{1}H NMR ($CDCl_3$, 400 MHz, 25 °C): δ 7.61 (bs, 2H, $H^{o''}$), 7.22 (bs, 1H, H^5), 7.12 (bs, 2H, $H^{m''}$), 6.29 (bs, 2H, $H^{4'}$), 6.25 (bs, 2H, NH_2), 2.69 (s, 6H, $Me^{5'}$), 2.32 (s, 3H, $Me^{''}$), 2.18 (s, 6H, $Me^{3'}$) ppm. ^{13}C{^{1}H} NMR ($CDCl_3$, 500 MHz, 25 °C): δ 158.9 (s, 1C, C^2), 157.1 (s, 2C, $C^{4,6}$), 150.9 (s, 2C, $C^{3'}$), 143.1 (s, 2C, $C^{5'}$), 128.8 (s, 2C, $C^{o''}$), 126.5 (s, 2C, $C^{m''}$), 123.0 (s, 2C, $C^{p''}$), 114.0 (s, 2C, $C^{4'}$), 86.0 (s, 1C, C^5), 21.4 (s, 1C, Me''), 15.7 (s, 2C, $Me^{5'}$), 14.9 (s, 2C, $Me^{3'}$) ppm. IR (Nujol): ν/cm^{-1} 3470, 3310 [ν(NH_2)], 1627, 784 [δ(NH_2)], 1581 [ν(CN/CC)], 1160 [ν(S−O)\, 1032, 1009, 815, 680, 566. UV−vis (CH_2Cl_2): λ (ε) 228 (10.1×10^4), 263 (9.1×10^4), 302 (5.4×10^4), 324 (6.5×10^4), 397 (2.1×10^4) nm. MS (FAB$^+$, NBA): *m*/*z* (rel intens %): 1444 [M^+ − bpz*apm − 2OTs, 0.3], 692 [M^+ − 2Cu − 2bpz*apm − 4OTs, 17.8], 629 [M^+ − 3Cu − 2bpz*apm − 4OTs, 32.9], 580 [M^+ − 2Cu − 3bpz*apm − 3OTs, 100], 517 [M^+ − 3Cu − 3bpz*apm − 3OTs, 26.7], 346 [M^+ − 3Cu − 3bpz*apm − 4OTs, 74.0] D.

[Cu(bpzpmpm)]$_4$(PF_6)$_4$ (9). To a solution of [$Cu(CH_3CN)_4$](PF_6) (82.4 mg, 0.221 mmol) in 10 mL of CH_2Cl_2 was added a solution of the ligand bpzmpm (50.0 mg, 0.221 mmol) in 10 mL of CH_2Cl_2. An orange precipitate appeared instantaneously and was stirred for 2 h, filtered off, and washed with THF (2 × 5 mL). After drying, an orange solid of **9**·$1.5CH_2Cl_2$ was obtained (78.4 mg, 0.168 mmol, 76%). Anal. Calcd for **9**·$1.5CH_2Cl_2$ ($C_{58}H_{72}N_{28}F_{24}P_4Cl_4Cu_4$): C, 33.45; H, 2.65; N, 20.58. Found: C, 33.67; H, 2.98; N, 20.59. ^{1}H NMR (acetone-d_6, 400 MHz, 25 °C): δ 9.01 (bs, 2H, $H^{5'}$), 8.60 (s, 1H, H^5), 8.27 (bs, 2H, $H^{3'}$), 7.06 (s, 2H, $H^{4'}$), 1.97 (s, 3H, Me_{pm}) ppm. ^{13}C NMR (acetone-d_6, 500 MHz, 25 °C): 168.9 (s, 1C, C^2), 160.4 (s, 2C, $C^{4,6}$), 144.7 (s, 2C, $C^{3'}$), 131.0 (s, 2C, $C^{5'}$), 112.8 (s, 2C, $C^{4'}$), 93.8 (s, 1C, C^5), 25.9 (s, 1C, Me_{pm}) ppm. ^{19}F NMR (acetone-d_6, 300 MHz, 25 °C): δ −73.3 (d, J = 703.5 Hz) ppm. IR (Nujol): ν/cm^{-1} 1595 [ν(CN/CC)], 844 [ν(P−F)], 558 [δ(P−F)]. MS (FAB$^+$, NBA): *m*/*z* (rel intens %): 1449 [M^+ − PF_6, 9.7], 515 [M^+ − 3Cu − 2bpzmpm − $4PF_6$, 30.7], 453 [M^+ − 3Cu − 3bpzmpm − $3PF_6$, 20.5], 289 [M^+ − 3Cu − 3bpz*apm − $4PF_6$, 100] D.

[Cu(bpzmpm)]$_4$(BF_4)$_4$ (10). The synthesis of **10** is similar to that of **9**. The amounts were as follows: 69.5 mg (0.221 mmol) of [$Cu(CH_3CN)_4$](BF_4) and 50.0 mg (0.221 mmol) of the ligand bpzmpm. Yield: 75.6 mg (0.186 mmol, 84%). Complex **10** is orange. Anal. Calcd for **10**·$1.5CH_2Cl_2$ ($C_{45.5}H_{43}B_4N_{24}F_{16}Cl_3Cu_4$): C, 33.45; H, 2.65; N, 20.58. Found: C, 33.67; H, 2.98; N, 20.59. ^{1}H NMR (acetone-d_6, 400 MHz, 25 °C): δ 9.03 (bs, 2H, $H^{5'}$), 8.60 (s, 1H, H^5), 8.27 (bs, 2H, $H^{3'}$), 7.06 (s, 2H, $H^{4'}$), 1.98 (bs, 3H, Me_{pm}) ppm. ^{19}F NMR (acetone-d_6, 300 MHz, 25 °C): δ −151.7 (s) ppm. IR (Nujol): ν/cm^{-1} 1595 [ν(CN/CC)], 1034, 1010 [ν(B−F)], 521 [δ(B−F)]. MS (FAB$^+$, NBA): *m*/*z* (rel intens %): 1419 [M^+ − BF_4, 9.0], 515 [M^+ − 3Cu − 2bpzmpm − $4BF_4$, 62.7], 289 [M^+ − 3Cu − 3bpzmpm − $4BF_4$, 100] D.

[Cu(bpzmpm)]$_4$(ClO_4)$_4$ (11). The synthesis of **11** is similar to that of **9**. The amounts were as follows: 72.3 mg (0.221 mmol) of [$Cu(CH_3CN)_4$](ClO_4) and 50.0 mg (0.221 mmol) of the ligand bpzmpm. Yield: 79.8 mg (0.190 mmol, 86%). Complex **11** is orange. Anal. Calcd for **11**·$1.5CH_2Cl_2$ ($C_{45.5}H_{43}N_{24}O_{16}Cl_7Cu_4$): C, 32.45; H, 2.57; N, 19.96. Found: C, 32.64; H, 2.66; N, 20.05. ^{1}H NMR (acetone-d_6, 400 MHz, 25 °C): δ 9.02 (bs, 2H, $H^{5'}$), 8.59 (s, 1H, H^5), 8.28 (bs, 2H, $H^{3'}$), 7.06 (s, 2H, $H^{4'}$) ppm. The pyrimidine Me resonance was not observed probably because of overlapping with the solvent. IR (Nujol): ν/cm^{-1} 1591 [ν(CN/CC)], 1102 [ν(Cl−O)], 623 [δ(Cl−O)]. MS (FAB$^+$, NBA): *m*/*z* (rel intens %): 1456 [M^+ − ClO_4, 9.0], 515 [M^+ − 3Cu − 2bpzmpm − $4ClO_4$, 100], 453 [M^+ − 2Cu − 3bpzmpm − $3ClO_4$, 11.8], 289 [M^+ − 3Cu − 3bpzmpm − $4ClO_4$, 95.0] D.

[Cu(bpzmpm)]$_4$(OTs)$_4$ (12). The synthesis of **12** is similar to that of **9**. The amounts were as follows: 88.2 mg (0.221 mmol) of [$Cu(CH_3CN)_4$](OTs) and 50.0 mg (0.221 mmol) of the ligand bpzmpm. Yield: 78.5 mg (0.157 mmol, 71%). Complex **12** is orange. Anal. Calcd for **12**·$2CH_2Cl_2$ ($C_{74}H_{72}N_{24}O_{12}S_4Cl_4Cu_4$): C, 44.14; H, 3.60; N, 16.69, S, 6.37. Found: C, 43.95; H, 3.78; N, 16.51, S, 6.21. IR (Nujol): ν/cm^{-1} 1595 [ν(CN/CC)], 1218, 1185, 1121 [ν(S−O)], 1034, 1010, 816, 682, 566. MS (FAB$^+$, NBA): *m*/*z* (rel intens %): 579 [M^+ − 2Cu − 2bpzmpm − 4OTs, 3.6], 526 [M^+ − 2Cu − 3bpzmpm − 3OTs, 22.1], 515 [M^+ − 3Cu − 2bpzmpm − 4OTs, 23.4], 289 [M^+ − 3Cu − 3bpzmpm − 4OTs, 100] D.

Cu(bpz*mpm)]$_4$(PF_6)$_4$ (13). To a solution of [$Cu(CH_3CN)_4$](PF_6) (66.0 mg, 0.177 mmol) in 10 mL of CH_2Cl_2 was added a

solution of the ligand bpz*mpm (50.0 mg, 0.177 mmol) in 10 mL of CH_2Cl_2. An orange suspension appeared instantaneously and was stirred for 2 h, filtered off, and washed with THF (2 × 5 mL). After drying, an orange solid of **13** was obtained (73.1 mg, 0.143 mmol, 81%). Anal. Calcd for **13**·CH_2Cl_2 ($C_{61}H_{74}N_{24}F_{24}P_4Cl_2Cu_4$): C, 29.11; H, 2.32; N, 17.81. Found: C, 29.24; H, 2.50; N, 17.55. ^{1}H NMR (acetone-d_6, 400 MHz, 25 °C): δ 8.00 (s, 1H, H^5), 6.64 (s, 2H, $H^{4'}$), 2.90 (s, 6H, $Me^{5'}$), 2.30 (s, 6H, $Me^{3'}$), 2.03 (s, 3H, Me_{pm}) ppm. ^{1}H NMR (acetone-d_6, 300 MHz, −80 °C): δ 8.03 (s, 1H, H^5), 6.69 (s, 2H, $H^{4'}$), 2.89 (s, 6H, $Me^{5'}$), 2.26 (s, 6H, $Me^{3'}$), 1.90 (s, 3H, Me_{pm}) ppm. ^{19}F NMR (acetone-d_6, 300 MHz, 25 °C): δ −73.2 (d, J = 703.5 Hz) ppm. ^{13}C{^{1}H} NMR (acetone-d_6, 500 MHz, 25 °C): δ 166.7 (s, 1C, C^2), 155.5 (s, 2C, $C^{4,6}$), 152.0 (s, 2C, $C^{3'}$), 144.8 (s, 2C, $C^{5'}$), 114.1 (s, 2C, $C^{4'}$), 94.2 (s, 1C, C^5), 26.5 (s, 1C, Me_{pm}), 14.5 (s, 2C, $Me^{5'}$), 14.1 (s, 2C, $Me^{3'}$) ppm. IR (Nujol): ν/cm^{-1} 1593, 1563 [ν(CN/CC)], 846 [ν(P−F)], 558 [δ(P−F)]. MS (FAB$^+$, NBA): m/z (rel intens %): 1817 [M^+ − PF_6, 10.9], 1672 [M^+ − 2PF_6, 1.5], 836 [M^+ − 2Cu − 2bpz*mpm − 3PF_6, 20.1], 774 [M^+ − 3Cu − 2bpz*mpm − 3PF_6, 2.8], 689 [M^+ − 2Cu − 2bpz*mpm − 4PF_6, 4.3], 627 [M^+ − 3Cu − 2bpz*mpm − 4PF_6, 29.7], 345 [M^+ − 3Cu − 3bpz*mpm − 4PF_6, 100] D.

[Cu(bpz*mpm)]$_4$(BF$_4$)$_4$ (14). The synthesis of **14** is similar to that of **13**. The amounts were as follows: 55.7 mg (0.177 mmol) of [Cu(CH_3CN)$_4$](BF_4) and 50.0 mg (0.177 mmol) of the ligand bpz*mpm. Yield: 62.6 mg (0.130 mmol, 74%). Complex **14** is orange. Anal. Calcd for **14**·2CH_2Cl_2 ($C_{62}H_{76}B_4N_{24}F_{16}Cl_4Cu_4$): C, 39.18; H, 4.03; N, 17.69. Found: C, 39.37; H, 3.76; N, 17.97. ^{1}H NMR (acetone-d_6, 400 MHz, 25 °C): δ 8.21 (s, 1H, H^5), 6.15 (s, 2H, $H^{4'}$), 2.74 (s, 6H, $Me^{5'}$), 2.25 (s, 6H, $Me^{3'}$), 2.03 (s, 3H, Me_{pm}) ppm. ^{19}F NMR (acetone-d_6, 300 MHz, 25 °C): δ −152.5 (s) ppm. IR (Nujol): ν/cm^{-1} 1591, 1561 [ν(CN/CC)], 1080, 1031 [ν(B−F)], 523 [δ(B−F)]. MS (FAB$^+$, NBA): m/z (rel intens %): 627 [M^+ − 3Cu − 2bpz*mpm − 4BF_4, 100], 432 [M^+ − 3Cu − 3bpz*mpm − 3PF_6, 5.5], 345 [M^+ − 3Cu − 3bpz*mpm − 4BF_4, 82.7], 283 [M^+ − 4Cu − 3bpz*mpm − 4BF_4, 39.4] D.

[Cu(bpz*apm)]$_n$Cl$_n$ (15). A suspension of 17.4 mg (0.176 mmol) of CuCl in 10 mL of acetone was added to a solution of 50.0 mg (0.176 mmol) of bpzpm in 10 mL of acetone. Immediately, a yellow solution was formed that was stirred at room temperature for 2 h. After this time, it was concentrated to 5 mL and washed with a mixture of CH_2Cl_2 and THF. The yellow solid of complex **15** was filtered and dried. Yield: 54.6 mg (0.128 mmol, 73%). Anal. Calcd for **15**·0.5CH_2Cl_2 ($C_{14.5}H_{18}N_7Cl_2Cu$): C, 41.00; H, 4.27; N, 23.08. Found: C, 41.22; H, 4.46; N, 23.32. ^{1}H NMR ($CDCl_3$, 400 MHz, 25 °C): δ 7.52 (bs, 1H, H^5), 6.10 (bs, 2H, $H^{4'}$), 5.82 (bs, 2H, NH_2), 2.69 (bs, 6H, $Me^{5'}$), 2.34 (bs, 6H, $Me^{3'}$) ppm. IR (Nujol): ν/cm^{-1} 3441, 3341, 3282 [ν(NH_2)], 1628, 1636, 794 [δ(NH_2)], 1585 [ν(CN/CC)], 224 [ν(Cu−Cl)]. UV−vis (CH_2Cl_2): λ (ε) 254 (8.0 × 10^4), 321 (6.9 × 10^4) nm. MS (FAB$^+$, NBA): m/z (rel intens %): 1210 [M^+ − bpz*apm − Cl, 1.6], 974 [M^+ − 2Cu − bpz*apm − 4Cl, 5.0], 692 [M^+ − 2Cu − 2bpz*apm − 4Cl, 5.5], 446 [M^+ − 2Cu − 3bpz*apm − 4Cl, 18.0], 629 [M^+ − 3Cu − 2bpz*apm − 4Cl, 15.4], 346 [M^+ − 3Cu − 3bpz*apm − 4Cl, 100] D.

[Cu(bpzapm)]$_4$(OTf)$_4$ (16). To a suspension of 21.8 mg of CuCl in 20 mL of acetone was added 50.0 mg (0.22 mmol) of bpzapm. The mixture was stirred at room temperature for 2 h. Then, 56.5 mg (0.22 mmol) of AgOTf was added. The brown suspension turned instantaneously into an orange suspension that was stirred at room temperature for 14 h and protected from light. AgCl was removed by filtration, the solution was evaporated to dryness, and the orange solid was washed with THF. Yield: 51.5 mg (0.117 mmol, 53%). Anal. Calcd for **16** ($C_{44}H_{36}N_{28}O_{12}F_{12}S_4Cu_4$): C, 30.04; H, 2.06; N, 22.29; S, 7.29. Found: C, 29.87; H, 2.18; N, 22.01; S, 7.59. ^{1}H NMR (acetone-d_6, 400 MHz, 25 °C): δ 8.99 (d, 2H, $J_{5'-4'}$ = 2.9 Hz, $H^{5'}$), 8.17 (d, 2H, $J_{3'-4'}$ = 1.7 Hz, $H^{3'}$), 8.15 (s, 1H, H^5), 7.00 (dd, 2H, $H^{4'}$), 5.99 (bs, 2H, NH_2) ppm. ^{19}F NMR (acetone-d_6, 300 MHz, 25 °C): δ −78.5 (s) ppm. ^{19}F NMR (acetone-d_6, 300 MHz, −80 °C): δ −79.9 (s) ppm. ^{13}C{^{1}H} NMR (acetone-d_6, 500 MHz, 25 °C): δ 158.8 (s, 1C, C^2), 157.0 (s, 2C, $C^{4,6}$), 144.8 (s, 2C, $C^{3'}$), 130.4 (s, 2C, $C^{5'}$), 112.7 (s, 2C, $C^{4'}$), 84.8 (s, 1C, C^5) ppm. IR (Nujol): ν/cm^{-1} 3469, 3344 [ν(NH_2)], 1628, 793 [δ(NH_2)], 1585 [ν(CN/CC)], 1260, 1263, 1219, 1162 [ν(S−O) or ν(C−F)], 636. MS (FAB$^+$, NBA): m/z (rel intens %): 1462 [M^+ − 2OTf, 0.7], 731 [M^+ − 2Cu − 2bpzapm − 3OTf, 7.9], 356 [M^+ − 2Cu − 3bpzapm − 4OTf, 51.7], 439 [M^+ − 3Cu − 3bpzapm − 3OTf, 50.9], 290 [M^+ − 3Cu − 3bpzapm − 4OTf, 100] D.

[Cu(bpz*apm)]$_4$(OTf)$_4$ (17). To a suspension of 74.8 mg of [Cu(bpz*apm)]$_n$(Cl)$_n$ (**15**·0.5CH_2Cl_2) in 30 mL of acetone (0.176 mmol) was added 45.2 mg (0.176 mmol) of AgOTf. An orange suspension was formed that was stirred at room temperature for 14 h and protected from light. Then, AgCl was removed by filtration, the solution was evaporated to dryness, and the orange solid was washed with THF. The complex was crystallized in acetone. Yield: 46.8 mg (0.092 mmol, 52%). Anal. Calcd for **17**·C_3H_6O ($C_{63}H_{74}N_{28}O_{13}F_{12}S_4Cu_4$): C, 37.06; H, 3.61; N, 19.21; S, 6.28. Found: C, 36.83; H, 3.42; N, 18.96; S, 6.05. ^{1}H NMR (acetone-d_6, 400 MHz, 25 °C): δ 7.44 (s, 1H, H^5), 6.62 (s, 2H, $H^{4'}$), 5.78 (s, 2H, NH_2), 2.87 (s, 6H, $Me^{5'}$), 2.25 (s, 6H, $Me^{3'}$) ppm. ^{19}F NMR (acetone-d_6, 300 MHz, 25 °C): δ −78.3 (s). ^{13}C{^{1}H} NMR (acetone-d_6, 500 MHz, 25 °C): δ 158.7 (s, 1C, C^2), 157.0 (s, 2C, $C^{4,6}$), 151.6 (s, 2C, $C^{3'}$), 144.3 (s, 2C, $C^{5'}$), 113.8 (s, 2C, $C^{4'}$), 86.7 (s, 1C, C^5), 14.6 (s, 2C, $Me^{5'}$), 13.9 (s, 2C, $Me^{3'}$) ppm. IR (Nujol): ν/cm^{-1} 3475, 3368 [ν(NH_2)], 1627, 787 [δ(NH_2)], 1585 [ν(CN/CC)], 1260, 1223, 1151 [ν(S−O) or ν(C−F)], 638. MS (FAB$^+$, NBA): m/z (rel intens %): 1055 [M^+ − Cu − 2bpz*apm − 2OTf, 7.7], 692 [M^+ − 2Cu − 2bpz*apm − 4OTf, 33.6], 629 [M^+ − 3Cu − 2bpz*apm − 4OTf, 62.6], 558 [M^+ − 2Cu − 3bpz*apm − 3OTf, 31.1], 495 [M^+ − 3Cu − 3bpz*apm − 3OTf, 8.4], 346 [M^+ − 3Cu − 3bpz*apm − 4OTf, 100] D.

[Cu(bpz*mpm)]$_4$(OTf)$_4$ (18). The synthesis of **18** is similar to that of **16**. The amounts were as follows: 17.5 mg (0.177 mmol) of CuCl, 50.0 mg (0.177 mmol) of the ligand bpz*mpm, and 45.5 mg (0.177 mmol) of AgOTf. Yield: 56.2 mg (0.113 mmol, 64%). Complex **18** is orange. The complex was crystallized in acetone. Anal. Calcd for **18**·1.5C_3H_6O ($C_{68.5}H_{81}N_{24}O_{13.5}F_{12}S_4Cu_4$): C, 39.81; H, 3.95; N, 16.26; S, 6.12. Found: C, 39.99; H, 3.82; N, 16.25; S, 5.98. ^{1}H NMR (acetone-d_6, 400 MHz, 25 °C): δ 8.01 (s, 1H, H^5), 6.62 (s, 2H, $H^{4'}$), 2.91 (s, 6H, $Me^{5'}$), 2.29 (s, 6H, $Me^{3'}$), 2.12 (s, 3H, Me_{pm}) ppm. ^{19}F NMR (acetone-d_6, 300 MHz, 25 °C): δ −80.1 (s). ^{13}C{^{1}H} NMR (acetone-d_6, 500 MHz, 25 °C): δ 166.7 (s, 1C, C^2), 155.5 (s, 2C, $C^{4,6}$), 151.8 (s, 2C, $C^{3'}$), 144.8 (s, 2C, $C^{5'}$), 113.9 (s, 2C, $C^{4'}$), 94.6 (s, 1C, C^5), 27.2 (s, 1C, Me_{pm}), 14.5 (s, 2C, $Me^{5'}$), 14.0 (s, 2C, $Me^{3'}$) ppm. IR (ATR): ν/cm^{-1} 1585 [ν(CN/CC)], 1259, 1220, 1145 [ν(S−O) or ν(C−F)]. MS (FAB$^+$, NBA): m/z (rel intens %): 841 [M^+ − 2Cu − 2bpz*mpm − 3OTf, 1.3], 627 [M^+ − 3Cu − 2bpz*mpm − 4OTf, 100], 345 [M^+ − 3Cu − 3bpz*mpm − 4OTf, 87.0] D.

Job Plot. Equimolar acetone-d_6 solutions of **6** (2.48 mM) and the guest were prepared and mixed in various ratios. ^{1}H and ^{19}F NMR spectra of the solutions were recorded, and changes in the chemical shifts of the resonance of the amine groups and the F atom of the BF_4^- anion were analyzed.

Binding Studies. The binding affinities were evaluated by NMR spectroscopy titrations. Titrations were performed in acetone-d_6 using a host concentration of 2.48 mM with varying amounts of tetrabutylammonium (TBA) salts. The chemical shifts were analyzed according to a 2:1 binding model, using the nonlinear least-squares curve-fitting program *HypNMR*.[28] For titrations of the free ligand, the concentration of L during the titrations of **6** in the presence of TBA(OTs) was used.

DOSY Experiments. The samples of **6** and **8** were prepared in acetone-d_6 with a 0.64 mM concentration. The TBAX salts were

(28) (a) Computer program: Gans, P. *HypNMR2006*; University of Leeds: Leeds, U.K., 2006. (b) Frassineti, C.; Ghelli, S.; Gans, P.; Sabatini, A.; Moruzzi, M. S.; Vacca, A. *Anal. Biochem.* **1995**, *231*, 374–382.

prepared in the same solvent with a 2.5 mM concentration. TMS was included in the samples as an internal reference material.[29]

General Procedure for the Anion-Exchange Experiments in the Solid State. A solution of two TBAX salts (0.015 M each one; X = BF_4 and OTf or PF_6) in 5 mL of THF was added over 0.064 mmol of the respective complex salt $[CuL]_4X_4$. The suspension obtained was stirred at room temperature during the specific time. The experiment of the column was carried out with a Pasteur pipet that was filled (L = 3 cm) with the solid. The solution of TBA salts was introduced into the pipet and freely allowed to pass by gravity. In all of the experiments, the solid was filtered and washed three times (3 × 5 mL) with THF. The ratio of anions in this product was determined by ^{19}F NMR as follows. Previously, equimolar amounts of TBA(PF_6), TBA(BF_4), and TBA(OTf) (0.0015 nmol of each) were solved in 0.5 mL of dimethyl sulfoxide (DMSO)-d_6, and the ^{19}F NMR spectrum was recorded at room temperture. The relative integration of the resonances was considered as a calibration of the NMR sensibility toward these anions. In each experiment, a sample of the obtained solid of anion exchange was solved in 0.5 mL of DMSO-d_6. The ^{19}F NMR spectrum was recorded, and the ratio of the anions was determined from integration of the different fluorinated anions conveniently corrected by the calibration coefficients.

Computational Methods. The geometry of the reported compounds was optimized using resolution of the identity MP2 (RI-MP2). The RI-MP2 method[30] applied to the study of anion−π interactions is considerably faster than MP2, and the interaction energies and equilibrium distances are almost identical for both methods.[31] Computations were performed using Dunning's correlation-consistent polarized valence basis sets of triple-ζ (aug-cc-pVTZ). For brevity, we will often refer to the aug-cc-pVTZ results by the shorthand notation AVTZ. In these calculations, a small-core pseudopotential and augmented correlation-consistent polarized valence triple-ζ (aug-cc-pVTZ-PP) basis set[32] was used for copper. The binding energies were calculated with and without correction for the basis set superposition error (BSSE) using the Boys−Bernardi counterpoise technique.[33] All RI-MP2 calculations were done within the frozen-core approximation.

The "atoms in molecules" (AIM)[34] analysis has been performed by means of the *AIM2000*, version 2.0,[35] program using the MP2/AVDZ//RI-MP2/AVTZ wave function. This methodology is useful for analyzing and relating the localization of critical points (CPs) and the calculation of electron densities and the Laplacian at these points with the strength of the ion−π[36] interactions and hydrogen bonding.[34a] Some basic concepts of Bader's topology analysis follow. The presence of a path linking two nuclei in an equilibrium structure implies that the two atoms are bonded to one another, and it is characterized by the bond CP (BCP), i.e., the point of minimum electron charge density (ρ) along the bond path but maximum along the direction perpendicular to the bond path. The two remaining stable CPs occur as a consequence of the particular geometrical arrangements of the bond paths, and they define the remaining elements of the molecular structure, i.e., rings and cages.

To evaluate the direction and magnitude of the donor−acceptor interactions, the natural bond orbital (NBO)[37] analysis was performed.[38] The donor−acceptor interactions are quantified by examining all possible interactions between filled (donor) Lewis-type NBOs and empty (acceptor) non-Lewis NBOs and by evaluating their energetic importance using the second-order perturbation theory in the NBO basis.[39] During interpretation of the results of such estimations, it should be noted that this approach is only performed at the self-consistent-field level of theory (i.e., the Fock operator is analyzed on the basis of the NBO), and only bonding interactions are considered (i.e., antibonding contributions are not covered by the NBO analysis and must be calculated separately).

All of the theoretical calculations described in this paper were carried out using *TURBOMOLE*, version 6.0,[40] and *Gaussian 03* programs.[41]

Results and Discussion

Synthesis and Characterization of the Ligands. Four new ligands were obtained from the reaction of the corresponding 4,6-dichloropyrimidine derivatives and an excess of sodium pyrazolate or 3,5-dimethylpyrazolate, using a method similar to that described for similar ligands[14,42] (see Chart 2).

A ligand containing 2-aminopyrimidine as the central ring bonded to two 2-pyridyl fragments has been previously reported,[43] and its coordination to silver centers leading to di- or polynuclear derivatives but not to grid complexes has been described.[44] Also, the ligand containing 2-methyl-4,6-(2-pyridine)pyrimidine has been previously

(29) Cabrita, E. J.; Berger, S. *Magn. Reson. Chem.* **2001**, *39*, S142–S148.
(30) (a) Feyereisen, M. W.; Fitzgerald, G.; Komornicki, A. *Chem. Phys. Lett.* **1993**, *208*, 359–363. (b) Vahtras, O.; Almlöf, J.; Feyereisen, M. W. *Chem. Phys. Lett.* **1993**, *213*, 514–518.
(31) (a) Frontera, A.; Quiñonero, D.; Garau, C.; Ballester, P.; Costa, A.; Deyà, P. M. *J. Phys. Chem. A* **2005**, *109*, 4632–4637. (b) Quiñonero, D.; Garau, C.; Frontera, A.; Ballester, P.; Costa, A.; Deyà, P. M. *J. Phys. Chem. A* **2006**, *110*, 5144–5148.
(32) Peterson, K. A.; Puzzarini, C. *Theor. Chem. Acc.* **2005**, *114*, 283–296.
(33) Boys, S. B.; Bernardi, F. *Mol. Phys.* **1970**, *19*, 553–566.
(34) (a) Bader, R. F. W. *Chem. Rev.* **1991**, *91*, 893–928. (b) Bader, R. F. W. *Atoms in Molecules. A Quantum Theory*; Clarendon Press: Oxford, U.K., 1990. (c) Bader, R. F. W. In *Encyclopedia of Computational Chemistry*; Schleyer, P. v. R., Allinger, N. L., Clark, T., Gasteiger, J., Kollman, P. A., Schaefer, H. F. S., III, Schreiner, P. R., Eds.; Wiley: Chichester, U.K., 1998; Vol. *1*, pp 64−86.
(35) http://www.AIM2000.de.
(36) Frontera, A.; Quiñonero, D.; Garau, C.; Ballester, P.; Costa, A.; Deyà, P. M.; Pichierri, F. *Chem. Phys. Lett.* **2006**, *417*, 371–377.
(37) (a) Weinhold, F. In *Encyclopedia of Computational Chemistry*; Schleyer, P. v. R., Allinger, N. L. T., Gasteiger Clark, J., Kollman, P. A., Schaefer, H. F. S., III, Schreiner, P. R., Eds.; Wiley: Chichester, U.K., 1998; Vol. *3*, pp 1792−1811. (b) Weinhold, F.; Landis, C. R. *Chem. Educ. Res. Pract. Eur.* **2001**, *2*, 91–104.
(38) Glendening, E. D.; Reed, A. E.; Carpenter, J. E.; Weinhold, F. *NBO 3.1 Program Manual*; 1988.
(39) (a) Reed, A. E.; Curtiss, L. A.; Weinhold, F. *Chem. Rev.* **1988**, *88*, 899–926. (b) Weinhold, F.; Landis, C. A. *Valency and Bonding: A Natural Bond Orbital Donor−Acceptor Perspective*; Cambridge University Press: Cambridge, U.K., 2005; p 760.
(40) Ahlrichs, R.; Bär, M.; Hacer, M.; Horn, H.; Kömel, C. *Chem. Phys. Lett.* **1989**, *162*, 165–169.
(41) Frisch, M. J.; Trucks, G. W.; Schlegel, H. B.; Scuseria, G. E.; Robb, M. A.; Cheeseman, J. R.; Montgomery, J. A., Jr.; Vreven, T.; Kudin, K. N.; Burant, J. C.; Millam, J. M.; Iyengar, S. S.; Tomasi, J.; Barone, V.; Mennucci, B.; Cossi, M.; Scalmani, G.; Rega, N.; Petersson, G. A.; Nakatsuji, H.; Hada, M.; Ehara, M.; Toyota, K.; Fukuda, R.; Hasegawa, J.; Ishida, M.; Nakajima, T.; Honda, Y.; Kitao, O.; Nakai, H.; Klene, M.; Li, X.; Knox, J. E.; Hratchian, H. P.; Cross, J. B.; Bakken, V.; Adamo, C.; Jaramillo, J.; Gomperts, R.; Stratmann, R. E.; Yazyev, O.; Austin, A. J.; Cammi, R.; Pomelli, C.; Ochterski, J. W.; Ayala, P. Y.; Morokuma, K.; Voth, G. A.; Salvador, P.; Dannenberg, J. J.; Zakrzewski, V. G.; Dapprich, S.; Daniels, A. D.; Strain, M. C.; Farkas, O.; Malick, D. K.; Rabuck, A. D.; Raghavachari, K.; Foresman, J. B.; Ortiz, J. V.; Cui, Q.; Baboul, A. G.; Clifford, S.; Cioslowski, J.; Stefanov, B. B.; Liu, G.; Liashenko, A.; Piskorz, P.; Komaromi, I.; Martin, R. L.; Fox, D. J.; Keith, T.; Al-Laham, M. A.; Peng, C. Y.; Nanayakkara, A.; Challacombe, M.; Gill, P. M. W.; Johnson, B.; Chen, W.; Wong, M. W.; Gonzalez, C.; Pople, J. A. *Gaussian 03*, revision C.01; Gaussian, Inc.: Wallingford, CT, 2004.
(42) Gómez-de la Torre, F.; de la Hoz, A.; Jalón, F. A.; Manzano, B. R.; Otero, A.; Rodríguez, A. M.; Rodríguez-Pérez, M. C. *Inorg. Chem.* **1998**, *37*, 6606–6614.
(43) Takagi, S.; Sahashi, T.; Sako, K.; Mizuno, K.; Kurihara, M.; Nishihara, H. *Chem. Lett.* **2002**, 628–629.
(44) Chi, Y.; Huang, K.; Cui, F. *Inorg. Chem.* **2006**, *45*, 10605–10612.

Scheme 1

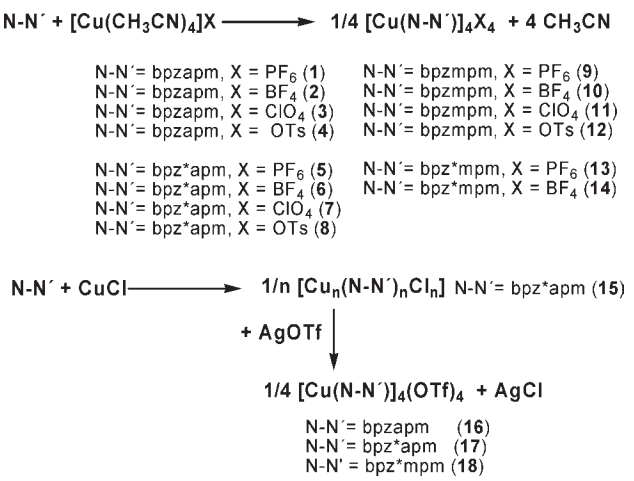

prepared[43] and proposed as a good chromogen for the detection of Cu^+ ions.[45b]

The ^1H and $^{13}C\{^1H\}$ NMR resonances of the new ligands were fully assigned thanks to NOE, NOESY, g-HMQC, and g-HMBC NMR spectra. In all cases, the existence of symmetric ligands with two equivalent pyrazolyl rings is observed.

Synthesis and General Characterization of the Complexes. The ligands were reacted with $[Cu(CH_3CN)_4]X$ in a 1:1 ratio (see Scheme 1). In the case of the triflate derivatives (OTf = CF_3SO_3), the ligand was reacted first with CuCl and afterward the chloride was eliminated by reaction with AgOTf. Only in the case of the ligand bpz*apm was the chloride derivative isolated.

The complexes are insoluble in hexane, diethyl ether, or THF and scarcely soluble in chloroform, dichloromethane, and acetone. In solutions of coordinative solvents such as DMSO, acetonitrile, or methanol, the resonances of the free ligands are detected by ^1H NMR spectroscopy, indicating decomplexation from the metal centers. Complexes with bpz*apm are more soluble in polar solvents such as acetone and dichloromethane.

The IR spectra reflect the presence of the expected functional groups. The stretching frequencies of the amino group of the free ligands are displaced toward higher numbers for the complexes, probably as a consequence of the existence of stronger hydrogen bonds in the free ligands. The characteristic stretching and deformation bands of the anions are observed.[46] For the BF_4^-, ClO_4^-, OTf^-, or OTs^- derivatives, the bands corresponding to the stretching modes are either broadened or split, an indication of a reduction in symmetry,[47] probably by interaction with the cations. However, the bands of the PF_6^- anion do not show an indication of symmetry reduction, probably as a consequence of weaker interactions of this anion with the cations. This is also the case for complex **11** with methylpyrimidine and ClO_4^-. It has been described that for triflate derivatives the appearance of a band around 1300 cm^{-1} indicates coordination of the anion to a metal center.[48] This band is not observed in the present work. For the chloride derivative **15**, a band due to a ν(Cu−Cl) vibration is observed at 224 cm^{-1}, a clear indication of coordination of the anion to the metal center.[46,49] Considering this fact, this complex probably does not have a tetranuclear grid structure and possibly exists as an oligomeric chain with chloride bridges.

In the MS spectra of the complexes (see the Experimental Section), the base peak is usually $[ML]^+$ (if not, this is of a high intensity), and for the tosylate or triflate derivatives, fragments of the type $[MLX]^+$ are, in general, more intense than those for the other anions, reflecting a higher anion-coordinating ability. Although of low intensity, peaks corresponding to fragments with three or four metal atoms are sometimes observed, and in some cases, the successive loss of anions is detected.

In order to better characterize our complexes, we have performed studies in the solid state that include X-ray diffraction analysis and a study of the anion interchange. The solution behavior was also analyzed by means of UV−vis and different NMR experiments that include diffusion studies and analysis of the anion interchange.

Solid-State Characterization. X-ray Structures of 3, 6, 7, 17, and 18. The molecular and crystalline structures of complexes **3**, **6**, **7**, **17**, and **18** have been determined by X-ray diffraction. The crystallographic data are given in Table 1, and a selection of bond distances and angles is gathered in Table 2. The corresponding ORTEP representations are reflected in Figures 1−4 except that of complex **7**, which is very similar to **6**. Both complexes only differ in the anion. All of the complexes exhibit a [2 × 2] grid structure comprising four copper(I) centers and four ligands. The cationic charge of the tetranuclear units is neutralized by four anions. Molecules of the included crystallization solvent are present in free spaces of the crystal lattices. As shown in Figures 1b, 3b, and 4b, two of the four counteranions are encapsulated in the two open voids formed in the tetracationic grids [when the two cavities are different, they are denoted as *u* (up) and *d* (down); the triflate anion in one void of complex **17** is disordered]. The other two anions are situated in intercationic positions in the crystal structure. Table 3 compiles some specific distances and angles that are important for the structure discussions. In this table, the data of two related complexes (**A** and **B**)[14] are included for the sake of comparison [**A** = $[Cu(bpzpm)]_4(BF_4)_4$, bpzpm = 4,6-bis(pyrazol-1-yl)-pyrimidine; **B** = $[Cu(bpz*pm)]_4(BF_4)_4$, bpz*pm = 4,6-bis-(3,5-dimethylpyrazol-1-yl)pyrimidine]. The geometry of the copper centers is distorted tetrahedral. The Cu−N distances lie in the normal range, and according to their relative basicities, they follow the order Cu−N(pm) > Cu−N(pz) > Cu−N(pz*) (see Table 2). The Cu−N(pm) distances are somewhat longer for the triflate derivatives **17** and **18**. The bite angles are very similar and range from 77.3 to 79.9° (Table 2). A much greater variety is found in the nonchelating angles with values from 104.8 to 146.4° (Supporting Information), a fact that reflects a

(45) (a) Hicks, R. G.; Koivisto, B. D.; Lemaire, M. T. *Org. Lett.* **2004**, *6*, 1887–1890. (b) Schilt, A. A.; Wu, F. J.; Case, F. H. *Talanta* **1976**, *23*, 543–545.
(46) Nakamoto, K. *Infrared and Raman Spectra of Inorganic and Coordination Compounds*, 4th ed.; John Wiley and Sons: New York, 1986; Part II.
(47) Beck, W.; Sunkel, K. *Chem. Rev.* **1988**, *88*, 1405–1421.
(48) (a) Lawrance, G. A. *Chem. Rev.* **1986**, *86*, 17–33. (b) Argouarch, G.; Hamon, P.; Toupet, L.; Hamon, J. R.; Lapinte, C. *Organometallics* **2002**, *21*, 1341–1348. (c) Stang, P. J.; Huang, Y. H.; Arif, A. M. *Organometallics* **1992**, *11*, 231–237.
(49) Troy, D.; Legros, J. P.; Maquillan, G. P. *Inorg. Chim. Acta* **1983**, *72*, 119–126.

Table 2. Selected Bond Distances (Å) and Bond Angles (deg) for the $[Cu_4L_4]^{4+}$ Cations of **3**, **6**, **7**, **17**, and **18**

3		**6**		**7**		**17**		**18**	
				Distances					
Cu1−N11	1.996(4)	Cu1−N11	1.971(2)	Cu1−N11	1.965(3)	Cu1−N11	1.991(2)	Cu1−N1	1.963(4)
Cu1−N21	2.009(4)	Cu1−N46	1.996(3)	Cu1−N46	1.995(4)	Cu1−N21	1.986(2)	Cu2−N7	1.982(4)
Cu1−N13	2.062(4)	Cu1−N13	2.081(2)	Cu1−N13	2.080(3)	Cu1−N13	2.119(2)	Cu1−N3	2.090(4)
Cu1−N23	2.083(4)	Cu1−N44	2.060(2)	Cu1−N44	2.064(3)	Cu1−N23	2.102(2)	Cu2−N4	2.105(4)
Cu2−N16	1.974(4)	Cu2−N16	1.968(2)	Cu2−N16	1.978(3)	Cu2−N16	1.970(2)	Cu2−N5	1.966(4)
Cu2−N31	2.019(4)	Cu2−N21	1.993(3)	Cu2−N21	1.994(4)	Cu2−N31	1.996(2)	Cu3−N11	1.972(4)
Cu2−N14	2.075(4)	Cu2−N14	2.083(2)	Cu2−N14	2.080(4)	Cu2−N14	2.150(2)	Cu2−N9	2.100(4)
Cu2−N33	2.045(4)	Cu2−N23	2.068(2)	Cu2−N23	2.066(3)	Cu2−N33	2.114(2)	Cu3−N10	2.111(4)
		Cu3−N26	1.973(2)	Cu3−N26	1.979(3)				
		Cu3−N31	1.965(3)	Cu3−N31	1.955(3)				
		Cu3−N24	2.077(2)	Cu3−N24	2.082(3)				
		Cu3−N33	2.081(2)	Cu3−N33	2.085(3)				
		Cu4−N36	1.965(2)	Cu4−N36	1.969(3)				
		Cu4−N41	1.981(2)	Cu4−N41	1.979(3)				
		Cu4−N34	2.085(2)	Cu4−N34	2.085(3)				
		Cu4−N43	2.075(2)	Cu4−N43	2.075(3)				
				Angles					
N11−Cu1−N13	79.8(1)	N44−Cu1−N46	78.82(9)	N44−Cu1−N46	78.8(1)	N21−Cu1−N23	77.69(8)	N1−Cu1−N3	79.3(2)
N21−Cu1−N23	79.6(1)	N11−Cu1−N13	78.34(9)	N11−Cu1−N13	78.1(1)	N11−Cu1−N13	77.91(8)	N4−Cu2−N5	78.4(1)
N31−Cu2−N33	79.2(1)	N21−Cu2−N23	78.65(9)	N21−Cu2−N23	78.6(1)	N31−Cu2−N33	78.29(8)	N7−Cu2−N9	78.3(2)
N14−Cu2−N16	79.9(1)	N14−Cu2−N16	78.39(9)	N14−Cu2−N16	77.9(1)	N14−Cu2−N16	77.34(8)	N10−Cu3−N11	79.0(2)
		N24−Cu3−N26	78.44(9)	N24−Cu3−N26	78.5(1)				
		N31−Cu3−N33	78.74(9)	N31−Cu3−N33	78.6(1)				
		N41−Cu4−N43	78.53(9)	N41−Cu4−N43	78.4(1)				
		N34−Cu4−N36	78.73(9)	N34−Cu4−N36	78.7(1)				

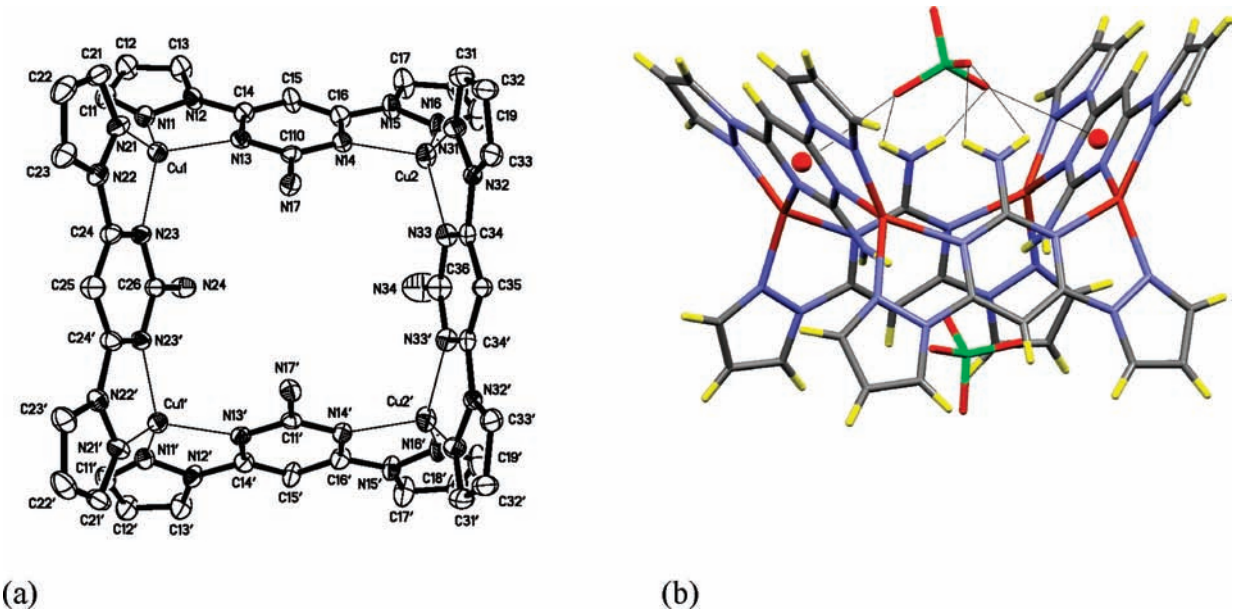

Figure 1. (a) ORTEP representation of the cation of **3**. Ellipsoids at a 20% level. (b) Stick representation of **3** including the encapsulated anions. Hydrogen bonds and anion−π interactions are indicated in the void *d*.

structural flexibility of the grids that is favorable for the encapsulation properties. The ligands, which exhibit normal bond lengths and angles, are approximately flat. However, important differences are found among them. In complexes with nonmethylated pyrazolyl groups (**3** and **A**), the ligands are more planar, with dihedral angles between the central pyrimidine and pyrazolyl rings ranging from 2.2 to 8.8°. Higher distortions are found in the derivatives with methylated pyrazoles, and values of this dihedral angle up to 18.0° (**17**) are found. In general, the pyrazolyl groups deviate from the pyrimidine plane to orientate the $Me^{5'}$ groups toward the inside of the cavity, a fact in relation with interactions with the encapsulated anion (see below).

Ideally a grid structure might adopt the point symmetry $-42m \equiv D_{2d}$. However, as indicated in Table 3, the molecular symmetry decreases in all of these examples.

The four copper centers in **3**, **17**, and **18** are perfectly coplanar [the root-mean-square (rms) deviation from the common least-squares plane is zero], and in **6** and **7**, some small deviation exists (the rms nonplanarity is 0.0381 Å for **6** and 0.0252 Å for **7**). They define a square with

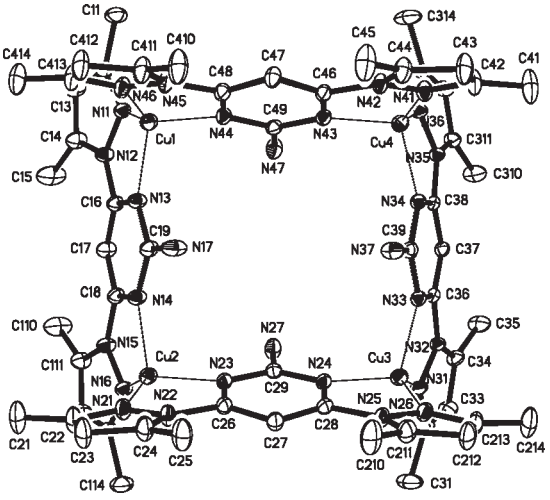

Figure 2. ORTEP representation of the cation of **6**. Ellipsoids at a 20% level. The atom numbering for **7** is the same.

Cu−Cu−Cu angles of nearly 90° and Cu−Cu distances of 6.1−6.3 Å but with values somewhat higher for the triflate derivatives (see Table 3). In the case of complex **B**, the four Cu atoms define a rhombus. As in the grids described previously by us with other pyrazolylpyrimidine ligands, including complexes **A** and **B**,[14] the faced ligands are not parallel but divergent, generating two groovelike cavities whose size is clearly dependent on the dihedral angle between each pair of ligands. To determine this angle, denoted as θ, the plane of the pyrimidine rings has been considered. In the case of the aminated derivatives, the value of θ is quite regular, between 40 and 50° (Table 3). Relatively small angles of 24.65° (**18***u* and -*d*) and 34.12° (**B***u* and -*d*) have been found for the derivatives containing methylated pyrazolyl rings but not amino groups. The explanation to these facts will be found when considering the interactions between the grids and the encapsulated counteranions. Clearly higher values for θ are found for **3***d* (67.4°) and **A***u* (76.9°), both containing ligands with nonmethylated pyrazolyl groups. The reason for this may be related to the fact that, in both derivatives, a partial interpenetration of two contiguous $[Cu_4L_4]^{4+}$ units that gives rise to intermolecular $\pi-\pi$ stacking contacts[50] between the inner sides of the pyrazole rings of two faced ligands is observed (see Figure 5a). This type of interpenetration has not been observed in complexes with methylated pyrazolyl groups, possibly for steric reasons. An intercationic $\pi-\pi$ stacking interaction but only involving one ligand per grid has been found in some voids: **3***u*, **6***u*, and **7***u*. However, apparently this has no effect on the angle θ (see Figure 5b).

There are two types of interactions between the counteranions found in the voids and the walls of the cavities of the cationic grids: hydrogen bonds[8,51] and anion$-\pi$ interactions[14,15] (see Chart 4 for the corresponding parameters). In the case of the aminated grids **3**, **6**, **7**, and **17**, all four NH groups are involved in hydrogen bonds with three atoms of the anions (O for ClO_4^- or OTf^- and F for BF_4^-; Figures 1b, 3b, and 4b, Chart 5, and Table 5), some of them bifurcated. In the case of **3**, with nonmethylated pyrazolyl groups, these are the only hydrogen bonds formed, but in derivatives with methylated pyrazoles (**6**, **7**, and **17**) in some voids, there are also hydrogen bonds involving Me^5 groups of the pyrazolyl rings (see Table 4). When the amino groups are not present (**18**, **A**, and **B**[14]), the hydrogen bonds are formed with Me or CH groups[8] of the pyrimidine rings and Me^5 groups of the pyrazolyl rings when present and usually involve less than three atoms of the anion. For the triflate derivatives, the F atoms also participate in the formation of hydrogen bonds. Interactions with the Me^5 groups are apparently the reason for deviation from planarity of the ligands and for reduction in the θ angle. In fact, when these interactions exist, the $Me^{5'}$ groups are deviated toward the inside of the cavity. However, the effect of these interactions is less marked for the aminated derivatives that exhibit, as stated, a more regular value for θ. Besides, it can be concluded, from the corresponding distances (Table 4), that the strongest hydrogen bonds are those involving the NH_2 groups and the weakest those formed with the Me^5 groups[8] in the aminated derivatives. All of these facts point to the idea that interactions with the amino groups play a main role in the aminated derivatives. The other hydrogen bonds are of minor importance in the stability of these host−guest complexes.

Anion$-\pi$ interactions are always present in both voids of all of the complexes involving the pyrimidine rings of the two faced ligands and two or three atoms of the anions (see Figures 1b, 3b, and 4b, Chart 5, and Table 4). In some cases, the same atom is involved in the hydrogen bonds and anion$-\pi$ interactions. A characteristic fact of the aminated derivatives is that usually one atom of each anion exhibits a d_{offset} (Chart 4) of a very small value (close to zero). In the case of **18**, the corresponding parameters do not allow us to conclude unequivocally that the anion$-\pi$ interaction is present. Considering that, we decided to perform computational studies to evaluate its existence (see below).

If we analyze the disposition of the anions in the cavities (OTf^- has also been considered as tetrahedral with a CF_3 substituent), the orientations found can be classified into two groups (see Table 5). In orientation **I**, one of the bonds is perpendicular to the drawing plane and it has only been found in **3***d*, the void with a high value of θ. In the case of orientation **II**, two bonds of the anion are in the drawing plane and the value of the angle α reflects the specific disposition of the anion. Thus, when α is small (**3***u*, **6***u*, **7***u*, and **17***u*, values up to 38°), three atoms point to the Cu_4 plane. The highest value (68.95°) is found for the nonaminated derivative **18**, where only one atom points to the inside of the cavity. Intermediate values are found for **6***d* and **7***d*, but in any case, three atoms of the anion interact with the amino groups. These facts reflect the tendency, already stated, to maximize the number of hydrogen bonds between the amino groups and the anions. The influence of the amino group can be clearly observed when the disposition of the OTf^- anion is compared in complexes **17** and **18**, which only differ in the presence of a NH_2 or Me group in the pyrimidine ring

(50) (a) Janiak, C. *Dalton Trans.* **2000**, 3885–3896 and references cited therein. (b) Ponzini, F.; Zagha, R.; Hardcastle, K.; Siegel, J. S. *Angew. Chem., Int. Ed.* **2000**, *39*, 2323–2325. (c) Kim, J. L.; Nilolov, D. B.; Burley, S. K. *Nature* **1993**, *365*, 520–527. (d) Kim, Y.; Geiger, J. H.; Hahn, S.; Sigler, P. B. *Nature* **1993**, *365*, 512–520.

(51) Jeffrey, G. A. *An Introduction to Hydrogen Bonding*; Oxford University Press: New York, 1997.

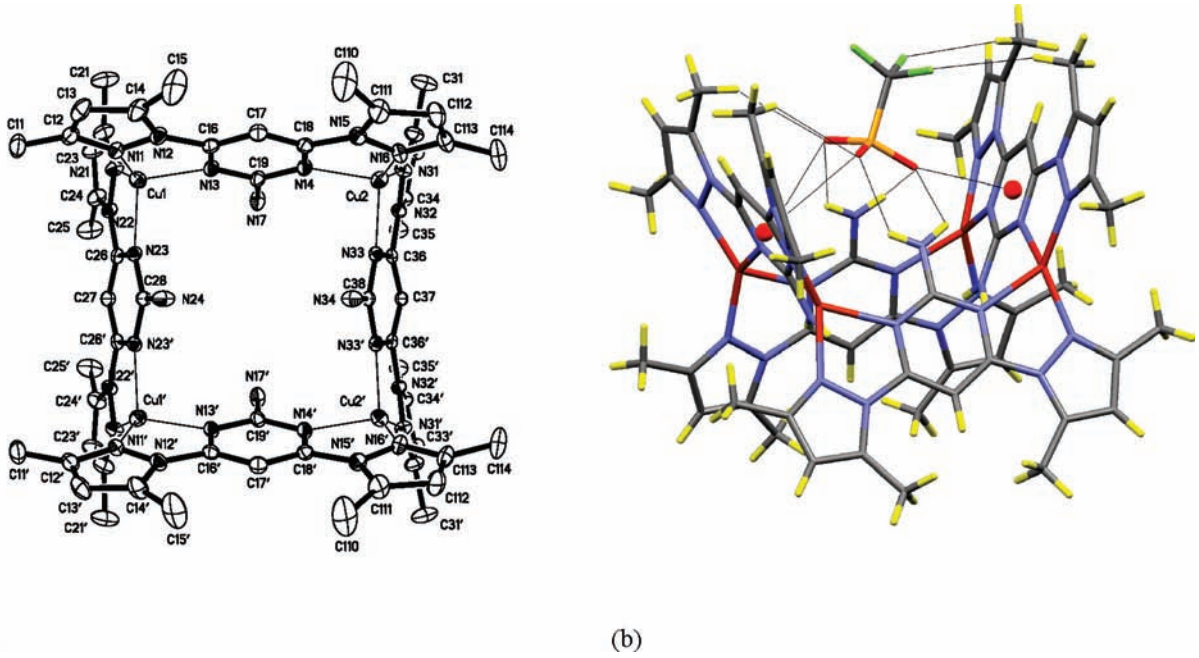

Figure 3. (a) ORTEP representation of the cation of **17**. Ellipsoids at a 20% level. (b) Stick representation of **17** including the encapsulated anions. Hydrogen bonds and anion−π interactions are indicated in the void *u*.

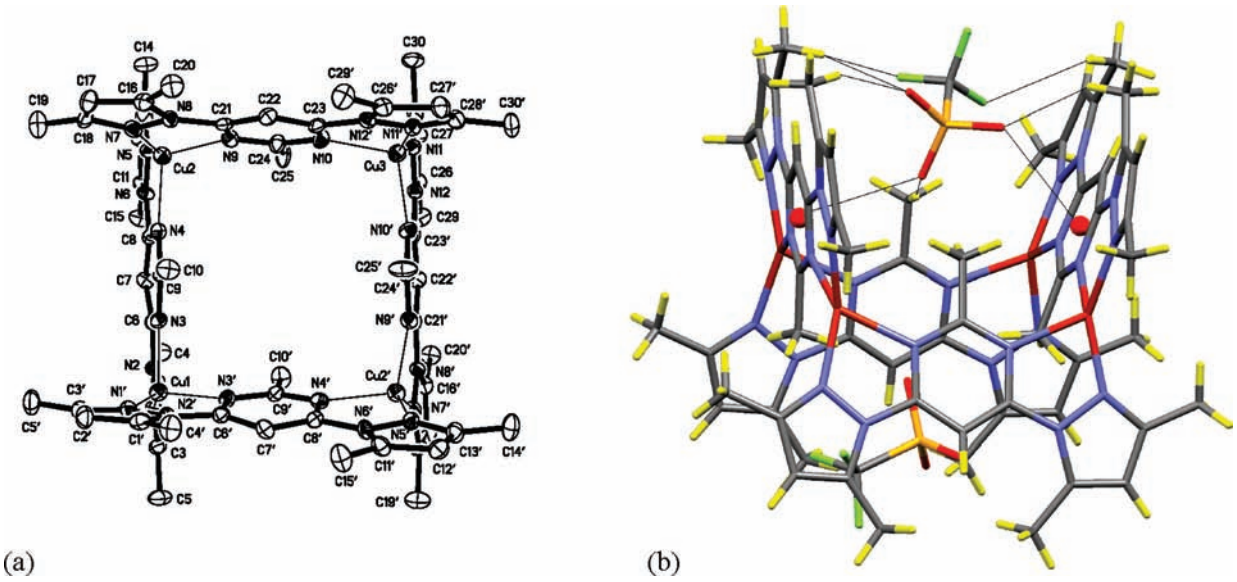

Figure 4. (a) ORTEP representation of the cation of **18**. Ellipsoids at a 40% level. (b) Stick representation of **18** including the encapsulated anions. Hydrogen bonds and anion−π interactions are indicated in one of the identical voids.

(Figures 3b and 4b). If penetration of the anion in the cavity is quantified considering the distance of the central atom of the anion to the plane Cu_4 (d_1, Table 5), it is seen that anions in the aminated derivatives penetrate less (this is also true when a comparison with the previously described nonaminated grids[14] is made). Evidently, this is due to the fact that the presence of the amino groups displaces the region in the cavity where the hydrogen bonds are formed. As a consequence, it can be stated that there is a clear influence of the presence of the amino groups in the disposition of the anions and in the pattern of the anion−cation interaction in the cavities.

Intermolecular interactions are also observed in these structures. They are of the following types: (i) $\pi-\pi$ stacking[50] (vide supra) and (ii) CH−π,[52] both between neighboring grids, and also (iii) weak hydrogen bonds involving CH groups[8] and (iv) anion−π interactions[14,15]

(52) (a) Kodama, Y.; Nishihata, K.; Nishio, M.; Nakagawa, N. *Tetrahedron Lett*. **1977**, *18*, 2105–2108. (b) Nishio, M.; Hirota, M. *Tetrahedron* **1989**, *45*, 7201–7245. (c) Nishio, M.; Umezawa, Y.; Hirota, M.; Takeuchi, Y. *Tetrahedron* **1995**, *51*, 8665–8701. (d) Takahashi, D. H.; Tsuboyana, S.; Umezawa, Y.; Honda, K.; Nishio, M. *Tetrahedron* **2000**, *56*, 6185–6191. (e) Nishio, M. *CrystEngComm* **2004**, *6*, 130–158. (f) Bogdanovic, G. A.; Spasojevic-de-Biré, A.; Zaric, S. D. *Eur. J. Inorg. Chem*. **2002**, 1599–1602. (g) Fujii, A.; Shibasaki, K.; Kazama, T.; Itaya, R.; Mikami, N.; Tsuzuki, S. *Phys. Chem. Chem. Phys*. **2008**, *10*, 2836–2843. (h) Nishio, M.; Hirota, M.; Umezawa, Y. *The C−H/π interaction evidence, nature, and consequences*; Wiley-VCH, Inc.: New York, 1998. (i) Quiocho, F. A.; Vyas, N. K. *Nature* **1984**, *310*, 381–386. (j) Vyas, N. K.; Vyas, M. N.; Quiocho, F. A. *Nature* **1987**, *327*, 635–638.

Table 3. Selected Geometric Parameters for the $[Cu_4L_4]^{4+}$ Cation of Complexes **3**, **6**, **7**, **17**, **18**, **A**, and **B**

complex	point symmetry of the $[Cu_4L_4]^{4+}$ unit	Cu−Cu distances [Å]	Cu−Cu−Cu angles [deg]	cavity	dihedral angles between rings in the ligand [deg]	θ [deg][a]	cavity size [Å] L; W [b]
3	$m \equiv C_s$	6.24	89.3 (2×)	*u*	2.15 (2×)	39.33	8.35; 6.53
		6.19 (2×)	90.7 (2×)		7.60 (2×)		
		6.08		*d*	6.77 (2×)	67.48	9.20; 6.17
					6.98 (2×)		
6	$1 \equiv C_1$	6.11 (2×)	90.2 (2×)	*u*	9.47 and 10.46	50.01	8.66; 6.37
		6.17 (2×)	89.8 (2×)		8.22 and 11.57		
				d	14.54 and 13.29	41.40	7.80; 5.87
					14.55 and 14.29		
7	$1 \equiv C_1$	6.12 (2×)	90.5 (2×)	*u*	9.30 and 10.28	48.47	8.69; 6.46
		6.17	89.4		9.39 and 11.62		
		6.16	89.5	*d*	14.80 and 13.02	40.68	7.78; 5.88
					14.43 and 14.72		
17	$m \equiv C_s$	6.30 (2×)	90.0 (4×)	*u*	17.98 (2×)	48.81	8.15; 5.90
		6.18 (2×)			7.48 (2×)		
				d	3.66 and 1.96 (2×)	40.10	8.06; 6.20
18	$2 \equiv C_2$	6.20 (2×)	89.73	*u* and *d*	3.06 and 13.30 (2×)	24.65 (2×)	7.62; 6.49
		6.21 (2×)	89.47		2.79 and 2.84 (2×)		
			90.40 (2×)				
A[c]	$m \equiv C_s$	6.027	90.36 (2×)	*u*	4.47 and 3.35 (2×)	76.92	9.43; 6.10
		6.103	89.64 (2×)	*d*	8.81 (2×)	41.45	8.49; 6.56
		6.145 (2×)			8.40 (2×)		
B[c]	$222 \equiv D_2$	6.106 (4×)	79.21 (2×)	*u* and *d*	4.51 and 12.51 (4×)	34.12 (2×)	7.82; 6.25
			100.79 (2×)				

[a] Angle between the opposite ligand planes. [b] See Chart 3 for the definition of L and W. [c] **A** = $[Cu(bpzpm)]_4(BF_4)_4$; **B** = $[Cu(bpz*pm)]_4(BF_4)_4$.

Chart 3

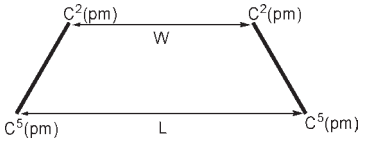

between grids and adjacent anions, not only those situated in intercationic positions but also those situated inside the cavities. Complementing the Coulombic forces between ions, all of these interactions must contribute to the stability of the crystals. A detailed analysis of all of these interactions is out of the scope of this work but could be obtained from the CIF files deposited as Supporting Information.

Anion-Exchange Experiments in the Solid−Liquid Interface. Inspired by the structural opening of these materials and by the ability of the cationic grids to interact with different anions (inside and outside the grid cavities), a set of experiments were carried out in order to demonstrate the mobility of the counteranions and the selectivity in the anion exchange in the solid−liquid interface and to evaluate the possible application of these materials as anion-exchange materials. Thus, suspensions of different solid samples of grid compounds ($[Cu(NN')]_4X_4$; X = PF_6^- or TfO^- and NN′ = aminated (bpzapm and bpz*apm) or nonaminated (bpzpm and bpz*pm) ligands)[14] were stirred with THF solutions of mixtures of BF_4^-, TfO^-, or PF_6^- as the TBA salts, as indicated in Scheme 2. In general, the complexes were previously obtained from precipitation after reaction of the copper salts and the ligands. In some cases, crystalline compounds were deliberately obtained (crystallinity confirmed by powder X-ray diffraction, results in parentheses in Table 6). The grid compounds are completely insoluble in THF. After a time of treatment, the solids were filtered, washed, and solved in DMSO and the ratio of the three different anions was analyzed by ^{19}F NMR spectroscopy (see Table 6).

According to these data, the following conclusions can be deduced:

(1) The results of entries 1−3 reflect that after 6 h the interchange process is complete.

(2) In the short contact time of an experiment when the ammonium salt solution is passed through a microcolumn filled with the copper complex (entry 4, see the Experimental Section), there is interchange, but the final equilibrium is not reached.

(3) A low selectivity toward a specific anion is observed. In any case, it changes with the presence of amino groups or methylated pyrazolyl rings (compare, for example, entries 2 and 9 or 6 and 7).

(4) The nature of the starting material influences the final result. For instance, the use of starting products with the same cation and different counteranions (compare entries 2 and 5 or 7 and 8) leads to different results. Furthermore, the crystalline structure is a decisive factor over the result of the anion interchange. Thus, when the two experiments of entry 8 are compared, it is observed that different data are obtained with the crystalline or precipitated derivative.

(5) The sample crystallinity is mostly preserved over the anion interchange process, but a change in the crystalline structure takes place. In the case of the processes of entries 7 and 8 (in parentheses), the samples of both starting materials and products were analyzed by powder X-ray diffraction and it was found that the four samples had different crystalline structures (see Figure S1 in the Supporting Information as an example).

Behavior in Solution. UV−vis. UV−vis spectra were recorded for dichloromethane solutions of the bpz*apm ligand and some of the complexes bearing this ligand, **5**−**8** and **15** (Experimental Section and Figure 6). It is very

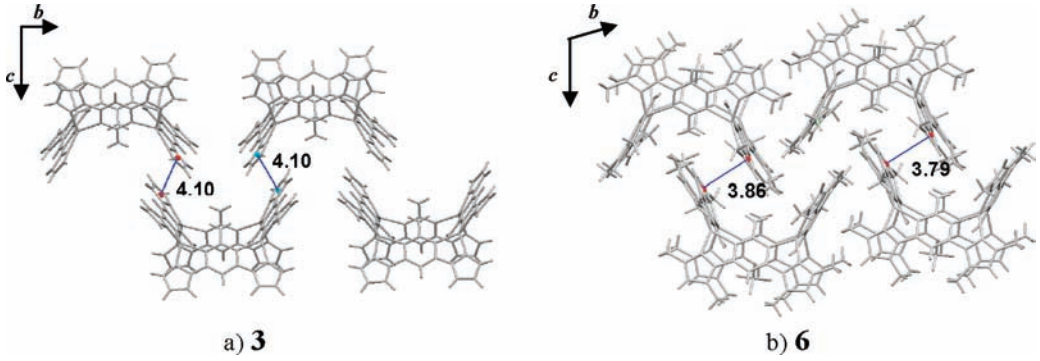

Figure 5. Packing in the crystal structure of grids **3** (a) and **6** (b) showing their interlacing. The centroid−centroid distances (Å) of the $\pi-\pi$ stacking interactions between pyrazole rings are indicated.

Chart 4

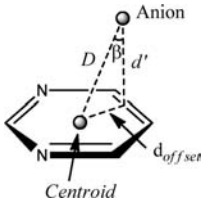

Chart 5. Anion−Cation Association through Hydrogen Bonds and Anion−π Interactions in Orientations **I** and **II** for the Aminated Derivatives[a]

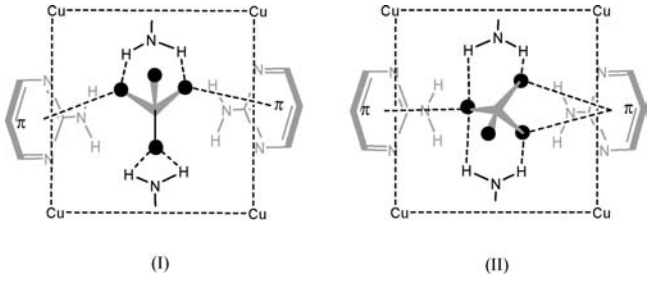

[a] The hydrogen bonds formed with the $Me^{5'}$ groups are not indicated.

illustrative to compare the spectra of the complexes with that of the free ligand. For the ligand, three bands are seen (223, 253, and 307 nm). For **5**−**8**, the band at 223 nm nearly disappears and the other two are slightly red-shifted. In addition, in these complexes, two new bands around 300 and 400 nm appear, with the latter being very broad and of low intensity. These bands are ascribed to metal-to-ligand charge transfer processes and are characteristic of copper(I) surrounded by four N atoms in a tetrahedral fashion.[53] All of these data are in accordance with the presence in solution of the grid complexes that do not dissociate ligands in a significant amount. A different situation is found for the complex with chloride, **15**, where the two characteristic bands of the complexes are not present and one at 254 nm is very close to that of the free ligand. The other ligand-centered band is less shifted to red than that in the other complexes (321 nm). All of this points to the fact that for **15** the tetranuclear grid either is not formed or at least is very much dissociated, with free ligand being a major component in solution. It is noticeable that the complex with OTs^-, **8**, is not dissociated in solution, which contrasts with the behavior of the analogous complex with the nonaminated ligand bpz*pm,[14] which showed clear evidence of dissociation. This difference in the stability of the grid may be related to the stronger interactions in the host−guest complex in **8** because of the formation of hydrogen bonds of the counteranion with the NH_2 groups.

NMR. The ^1H and $^{13}C\{^1H\}$ NMR spectra of the complexes (the high insolubility of some complexes prevented the recording of some spectra; see Experimental Section) were assigned using the same techniques as those indicated for the ligands. Symmetric and single ligands are observed in all cases. This could reflect either that the expected grid structure is maintained or that dynamic processes involving grid rupture exist in solution. This second possibility is considered less likely, taking into account the UV−vis data and the fact that no changes in the N-donor ligand were observed in the ^1H NMR spectra at low temperature (−80 °C, obtained for the more soluble complexes **5**, **6**, **7**, **8**, **13**, and **17**). In the case of complex **8**, at −80 °C, broadening of the OTs^- anion resonances was observed, indicating the possible existence of anion interchange in solution on the time scale of the NMR spectroscopic measurement.

Coordination of the ligands can be inferred from the change in the chemical shift of the resonances with respect to the free ligand. More specifically, the following are observed: (i) a shift to lower field of the pyrazole proton resonances, (ii) a shift to higher or lower field (methylated or nonmethylated pyrazolyl rings, respectively) of the pyrimidine H^5 proton signals, and (iii) a shift to higher field of the pyrimidine Me^2 and NH_2 resonances. The change observed for the amino resonances reflects the presence of weaker hydrogen bonds in the complexes with respect to the free ligands. If the resonances of a set of derivatives with the same ligand and different anions are compared (bpz*apm ligand and derivatives **5**, **6**, **7**, **8**, and **17**), similar chemical shift changes are found except for the OTs^- (**8**) derivative, a fact that could indicate stronger interactions of this anion with the grid. A special case is the chloride derivative **15**. In this complex, the resonances are much more similar to those of the free ligand than in the other derivatives, a fact that could be due to a competition between the ligand and the chloride toward coordination

(53) (a) Ziessel, R.; Charbonnière, L.; Cesario, M.; Prangé, T.; Nierengarten, H. *Angew. Chem., Int. Ed.* **2002**, *41*, 975–979. (b) Lan, Y.; Kennepohl, D. K.; Moubaraki, B.; Murray, K. S.; Cashion, J. D.; Jameson, G. B.; Broker, S. *Chem.—Eur. J.* **2003**, *9*, 3772–3784.

Table 4. Representative Distances for the Hydrogen Bonds and Anion−π Interactions (Å) of the Anions and the $[Cu_4L_4]^{4+}$ Units in Complexes **3**, **6**, **7**, **17**, and **18**

		heteroatom−heteroatom distances for the hydrogen bonds				anion−π	
complex/ cavity		terminal O(F)···NH_2	bifurcated H_2N···O(F)···NH_2	terminal O(F)···CH_3	bifurcated H_3C···O(F)···CH_3	$D_{O(F)\cdots centroid}$	d_{offset}[a]
3	*u*	2.97 (2×)	3.09 (2×)			3.19	0.08
						3.45 (2×)	1.70
	d	3.04 (2×)	2.77			3.08 (2×)	0.37
6	*u*	2.84	3.14			3.34	0.23
		2.84	3.14			3.26	1.30
						3.28	1.34
	d	3.09	2.93	3.61	3.92, 3.80	2.85	0.13
		2.99	3.17	3.64		3.32	1.47
						3.39	1.49
7	*u*	2.92	3.17			3.39	0.08
		2.93	3.20			3.29	1.37
						3.32	1.44
	d	3.05	3.00	3.54	3.72, 3.79	2.85	0.18
		3.14	3.05	3.55		3.42	1.58
						3.44	1.60
17	*u*	2.97 (2×)	3.18 (2×)	3.67 (2×) (OC)		2.87	0.18
				3.74 (2×) (FC)		3.31 (2x)	1.43
	d			disordered			
18	*ud*			3.25 (OC)	3.35 (COC)	4.06	2.99
				3.21 (FC)	3.57 (COC)	3.26	0.84
				3.37 (FC)		3.49	1.81
						4.09	0.37

[a] See Chart 4 for the definition of d_{offset}

Table 5. Orientation of the Anions in the Cavities of Complexes **3**, **6**, **7**, **17**, and **18** and Some Geometrical Parameters

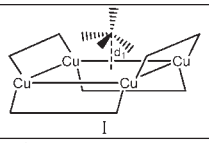

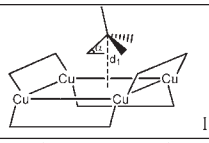

Complex cavity	**3***d*	**3***u*	**6***u*	**6***d*	**7***u*	**7***d*	**17***u*	**18***ud*
α [deg] [a]	2.30	36.82	29.10	57.28	29.29	59.42	38.10	68.95
d_1 [Å]	3.44	3.61	3.44	3.55	3.52	3.57	3.45	3.88
θ [deg] [b]	67.48	39.33	50.01	41.40	48.47	40.68	48.81[c]	24.65

[a] See **II** for the definition of α. In orientation **I**, α is the angle between the anion bond that points at the viewer and the Cu_4 plane. [b] Dihedral angle between opposite ligand planes. [c] 40.10 for **17***d*.

Scheme 2

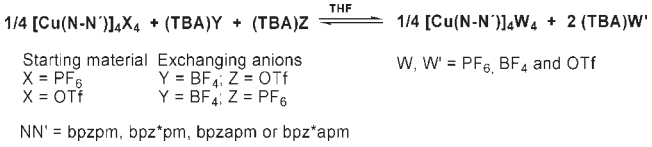

Table 6. Anion Composition (%) of the Products Obtained from the Solid−Liquid Anion-Exchange Experiments

			anion (%)[a]		
entry	starting complex	reaction time	PF_6^-	BF_4^-	OTf^-
1	$[Cu(bpz*pm)]_4(PF_6)_4$	6 h	41	31	28
2		24 h	41	31	28
3		7 days	42	31	27
4		column	53	24	24
5	$[Cu(bpz*pm)]_4(OTf)_4$	24 h	38	46	16
6	$[Cu(bpzpm)]_4(PF_6)_4$	24 h	60	25	15
7	$[Cu(bpzapm)]_4(PF_6)_4$ (**1**)	24 h	13 (13)	43 (44)	44 (43)
8	$[Cu(bpzapm)]_4(OTf)_4$ (**16**)	24 h	66 (33)	22 (41)	12 (26)
9	$[Cu(bpz*apm)]_4(PF_6)_4$ (**5**)	24 h	28	54	18

[a] In parentheses are the results obtained from crystallized samples.

to the copper(I) centers, and this is in accordance with the special behavior found for this derivative by UV−vis.

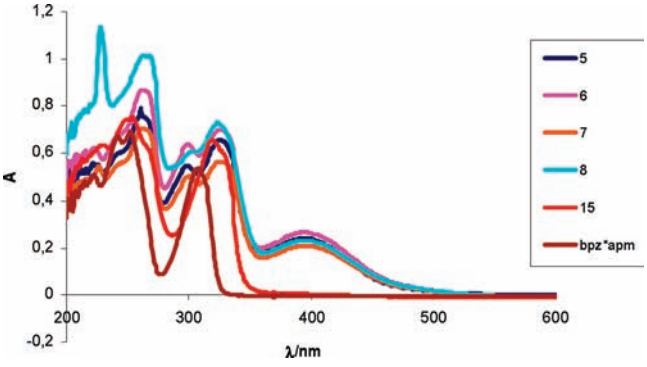

Figure 6. UV−vis spectra of complexes **5**−**8** and **15** and the ligand bpz*apm in CH_2Cl_2.

The ^{19}F NMR spectra reflect the presence of the fluorine-containing anions that give rise to single resonances. These signals are, in general, sharp at room temperature and also at −80 °C (the complexes studied were **1**, **2**, **5**, **16**, and **17**). However, for **6**, the BF_4^- signal is broad at both room and low temperature, suggesting the presence of a relatively slow exchange process involving the anion.

Study of the Cation−Anion Interactions in Solution. DOSY NMR spectroscopy is a fast and easy method to

Table 7. Values of Diffusion Coefficients for Complexes **5**, **6**, **8**, and **13** (D_{grid}), for Their Counteranions (D_{anion}), for the Anions as TBAX Salts ($D_{anion\ salt}$), and for TMS (D_{TMS}) as an Internal Reference[a]

	5	**6**	**8**	**13**
[complex] (mM)	0.634	0.634	0.635	0.634
D_{grid} (^{1}H)	10.56 ± 0.02	8.91 ± 0.02	7.77 ± 0.02	11.67 ± 0.02
D_{anion}	20.62 ± 0.03 (^{19}F)	19.677 ± 0.03 (^{19}F)	10.419 ± 0.03 (^{1}H)	23.57 ± 0.03 (^{19}F)
D_{TMS} (^{1}H)	32.429 ± 0.03	32.429 ± 0.03	31.089 ± 0.03	32.429 ± 0.03
D_{grid}/D_{TMS}	0.3256 ± 0.009	0.2747 ± 0.009	0.2499 ± 0.009	0.3599 ± 0.009
D_{anion}/D_{TMS}	0.6358 ± 0.0015	0.6068 ± 0.0015	0.3352 ± 0.0013	0.7268 ± 0.0016
$D_{anion\ salt}$	29.72 ± 0.03	34.835 ± 0.03	17.504 ± 0.03	29.71 ± 0.03
$D_{anion\ salt}/D_{TMS}$	0.9164 ± 0.0018	1.0743 ± 0.0019	0.5629 ± 0.0015	0.9161 ± 0.0018
ρ	0.4749 ± 0.0044	0.5847 ± 0.0034	0.7276 ± 0.0099	0.3404 ± 0.0043

[a] D values are listed as 10^{-10} m^2 s^{-1}. T = 298 K.

establishing the binding between guests and hosts. Diffusion coefficients are sensitive to the structural properties of the observed species such as molecular weight, size, and shape and also to binding processes and molecular interactions.[54] In the present case, diffusion NMR experiments were carried out for complexes **5**, **6**, **8**, and **13**, as an additional approach to investigating the cation−anion interactions in solution. Diffusion coefficients were determined for the tetracationic entities (^{1}H measurements) and for their counteranions (^{1}H and ^{19}F measurements) in dilute acetone-d_6 solutions (< 1 mM of the grids). The coefficients for the free anions were determined from solutions of TBAX (TBA = tetrabutylammonium; X = BF_4^-, OTs^-, and PF_6^-) salts at similar concentrations. The values (Table 7) were smaller for the anions in the complexes (they diffused more slowly) than for the classical salts at similar concentrations but higher than the values of the grids. These data suggest that the anions are not completely retained by the grids in solution but do exhibit some kind of dynamic association.

Assuming that the observed diffusion coefficients for the grids are similar to those expected for the complexed anions, the fraction of bound anions (ρ; Table 7) can be obtained from the following equation:

$$D_{obs} = \rho D_{complex} + (1 - \rho) D_{free}$$

where $D_{complex}$ is the diffusion coefficient obtained for the grid, D_{free} is that of the anion in the classical salt, and D_{obs} is the observed value (fast exchange situation) for the anions that should be the weighed average value of $D_{complex}$ and D_{free}.

The values for the fraction of bound guest (ρ) are shown in Table 7. It is concluded that ρ is higher for the aminated derivatives. In fact, the values for **5**, **6**, and **8** are higher than that of **13** and also those of previously reported nonaminated grids. When $[Cu(bpz^*pm)]_4(BF_4)_4$[14] is compared to **6**, which only differ in the presence of the amino group, the value of 0.34 changes to 0.58. The comparison of the values of **5** or **6** and **8** indicates that OTs^- is bonded more strongly to the cationic grid compared to the BF_4^- or PF_6^- anions.

Consequently, the presence of functional groups such as NH_2 or of counteranions that can give rise to stronger interactions increases the stability of the host−guest complexes.

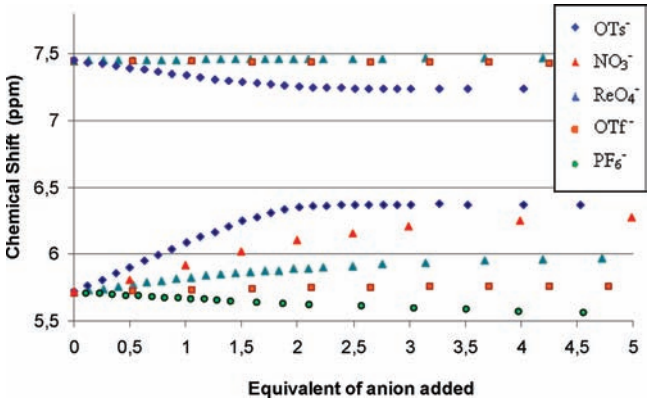

Figure 7. ^{1}H NMR monitoring of the chemical shift of the NH_2 (5.72 ppm) and H^5 pyrimidine (7.45 ppm) resonances of **6** upon the addition of a range of TBA salts in acetone-d_6. For PF_6^- and NO_3^-, the data for the NH_2 resonance are not included because they are similar to those of OTf^- or ReO_4^-.

NMR experiments where the anion interchange in solution was analyzed were also performed. The chemical shift evolution of a number of proton resonances and also that of the BF_4^- anion were studied respectively by ^{1}H and ^{19}F NMR spectroscopic titration of **6** with increasing amounts of TBAX salts in an acetone solution (X = OTs^-, NO_3^-, ReO_4^-, OTf^-, and PF_6^-; see Figures 7 and 8).

In Figure 7, the evolution of the chemical shift of the NH_2 and H^5_{pm} resonances is shown. The H^5_{pm} signal is shielded when the OTs^- salt is added, suggesting that the ring electronic density of the anion may be affecting this proton. For the NH_2 resonance, a shift is observed [except for the addition of TBA(OTf)] when the salts are added, indicating that some cation−anion interaction exists. This effect may be illustrative of the intensity of the NH···D hydrogen bond (D = O and F) established with the different counteranions. As depicted in Figure 7, anions such as OTs^-, NO_3^-, and ReO_4^- shift the resonance to lower field, OTf^- has practically no effect, and PF_6^- produces a shift to higher field. These data indicate that, in the absence of more important effects, the hydrogen bond strength would follow the order $OTs^- > NO_3^- > ReO_4^- > BF_4^- \approx OTf^- > PF_6^-$. This conclusion fits with the principle that the complex stability increases with greater Brønsted basicity of the guest and with the results previously reported.[55] Another experiment was carried

(54) (a) Price, W. *Concepts Magn. Reson.* **1997**, *9*, 299–336. (b) Price, W. *Concepts Magn. Reson.* **1998**, *10*, 197–237. (c) Johnson, C. S., Jr. *Prog. NMR Spectrosc.* **1999**, *34*, 203–256. (d) Cohen, Y.; Avram, L.; Frish, L. *Angew. Chem., Int. Ed.* **2005**, *44*, 520–554.

(55) Kelly, T. R.; Kim, N. H. *J. Am. Chem. Soc.* **1994**, *116*, 7072–7080.

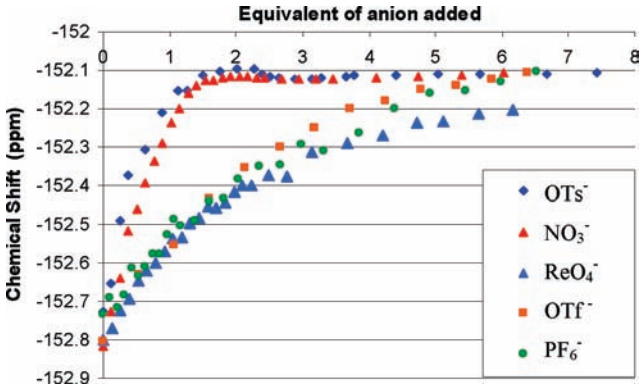

Figure 8. Plot representation for complex **6** of the change observed in the chemical shift of the BF_4^- resonance (^{19}F NMR) upon the addition of a range of TBAX salts in an acetone-d_6 solution.

out to evaluate if there were hydrogen bonds between the free ligand, bpz*apm, and the salt TBA(OTs). An acetone-d_6 solution of TBA(OTs) (1−6 equiv) was added to a solution of the free ligand (at the same concentration as that in the experiment with complex **6**), and no change in the chemical shift of the ligand was observed. It was concluded that it is the grid $\mathbf{6}^{4+}$ and not the free ligand that acts as a receptor of the OTs^- anions.

The effect of the salt addition was also followed by ^{19}F NMR spectroscopy. The ^{19}F NMR resonance of BF_4^- in **6** is, as stated, broad and slightly shielded (−152.8 ppm) compared with that of TBA(BF_4) (−152.1 ppm). This fact points to the existence of some cation−anion interaction in solution. This assumption is supported by the effect of the addition of TBAX salts to the solution of **6**: the chemical shift of the BF_4^- resonances changes and approaches that of the free anion (see Figure 8), and the signals progressively sharpen. It is concluded that the chemical shift exhibited by the anion in complex **6** is an average of the free and interacting anions, reflecting a fast exchange process (see Figures S2−S4 in the Supporting Information, where a comparison with the addition of PF_6^- is included). As is reflected in Figure 8, the affinity toward OTs^- and NO_3^- is higher than that of the rest of the anions. It is also observed that the sharpening of the resonance is especially pronounced, and only after the addition of these two anions is the resolution high enough to distinguish the two isotopomers of BF_4^-. Besides, the fact that the chemical shift of the free BF_4^- is reached, for these two anions, after the addition of 2 equiv of the salt suggests a high stability of the grid−X_2 complexes with respect to the initial species, **6**.

The stoichiometry of the complex formed with OTs^- and the grid of **6** was confirmed by a Job plot obtained from the chemical shifts of the NH_2 and BF_4^- groups (by ^1H and ^{19}F NMR spectroscopy, respectively) after the addition of TBA(OTs) to **6**. In both experiments, the curve maximum occurs at 0.33 molar fraction of host, which is indicative of a 1:2 (host−guest) stoichiometry, demonstrating that both sides of the host molecule are able to complex the OTs^- anion.

Data from Figure 7 have been used to calculate the association constants, K_{11} and K_{12} (Table 8), for formation of the 1:1 and 1:2 adducts (see Scheme 3) by nonlinear least-squares regression using the program *HypNMR-2006*.[28] Strong binding in a 1:2 ratio is observed for both

Table 8. K_{11} and K_{12} Data Obtained upon the Addition of TBA Salts over **6** in Acetone-d_6

TBAX	log K_{11}	log K_{12}
X = OTs^-	>4[a]	>4[a]
X = NO_3^-	3.69(4)	3.24(4)
X = ReO_4^-	2.56(3)	
X = PF_6^-	<10	
X = OTf^-	2.74 (10)	

[a] Too high to determine reliably by NMR spectroscopic titration.

Scheme 3

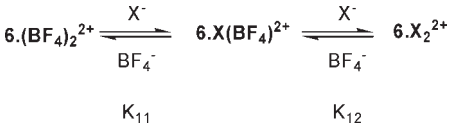

Chart 6. Pyrimidine **c1** and its Copper(I) Complex **c2**

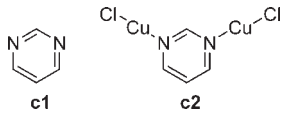

Table 9. Geometrical Parameters (D, d', and d_{offset} in Angstroms and β in Degrees, As Described in Chart [4]) and Interaction Energies without and with BSSE Correction (E and E_{CP}, in kcal mol^{-1}, Respectively) at the RI-MP2/AVTZ Level of Theory

		RI-MP2/AVTZ					
compound	interacting atom	D	d'	d_{offset}	β	E	E_{CP}
c3	O4	3.612	2.871	2.192	37.36	−7.04	−5.87
	O6	3.972	3.941	0.495	7.16		
c4	O4	3.639	2.838	2.278	38.75	−26.64	−25.20
	O6	3.936	3.900	0.531	7.76		
X-ray	O4	3.489	2.982	1.811	31.27		
	O6	4.087	4.069	0.383	5.38		

tosylate and nitrate anions, while the less basic anions form weaker 1:1 complexes. The negative chemical shift change for PF_6^- implies that this anion is bound extremely weakly, and no reliable binding constant was obtained. The lower values of K_{12} compared to K_{11} for nitrate imply that the binding of the first anion to one face of the grid somewhat inhibits the binding of a second anion. Possibly the reason may be the decrease of the Coulombic attractions between the anion and a cation with a lower positive charge. The very strong values obtained for tosylate are surprising and may imply a significant $\pi-\pi$-stacking component to the binding. Attempts were also made to refine binding constants from the ^{19}F NMR spectroscopic data, but consistent values were not obtained. However, the steeper slope of the plots of tosylate and nitrate is broadly consistent with the conclusions from the ^1H NMR spectroscopic data.

Computational Studies. The existence of anion−π interactions in the cavities of complex **18** was evaluated by means of theoretical studies in model compounds from a fragment taken from the X-ray structure to allow a direct comparison. As a model π system, we have chosen the pyrimidine ring either not coordinated, **c1**, or coordinated, **c2**, to two Cu^ICl metal centers (Chart 6). As the anion−π-interacting molecule, we considered triflate

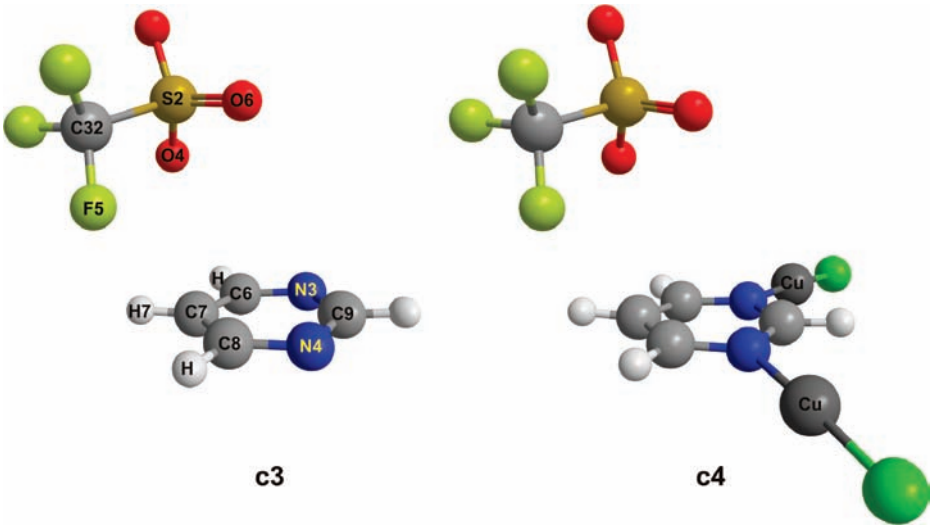

Figure 9. RI-MP2/AVTZ-optimized structures of complexes **c3** and **c4** and atom labeling. Distances are in angstroms.

without simplifications because the F atoms might play an important role. Selected intermolecular distances and a dihedral angle were kept frozen in the complexes to keep both CuCl and OTf^- groups as they are in the X-ray structure. We have optimized the geometry of the complexes at the RI-MP2/AVTZ level of theory. Their binding energies without and with BSSE correction (E and E_{CP}, respectively) and selected geometrical parameters are summarized in Table 9.

The interaction energies for complexes **c3** and **c4** are negative (see Figure 9 for the optimized pyrimidine/triflate complexes). It is noticeable that **c4** has a larger binding energy (-25.20 kcal mol^{-1}) than **c3** (-5.87 kcal mol^{-1}). This is due to coordination of copper(I) to pyrimidine, which dramatically changes the π acidity of the ring, as was already noticed for coordination of zinc(II) to *s*-triazine[56] and silver(I) to either pyridine or pyrazine.[57]

In principle, we can consider the possibility that two O atoms could be anion$-\pi$ interacting with the aromatic system, namely, O4 and O6 atoms (see Figure 9). From an inspection of the results (Table 9), the existence of the anion$-\pi$ interaction in our complexes for both O4 and O6 is uncertain, according to Reedjik criteria;[15l] for O4, although both D and d' distances have reasonable values for an anion$-\pi$ interaction, the d_{offset} distance and the β angle are quite large (see Chart 4). For O6, although both d_{offset} and β are within the reported values,[15l] the distances from O4 to the centroid, D, and to the plane defined by the ring, d', have borderline values, ca. 4 Å. In order to shed some light on the existence of anion$-\pi$ interaction in our system, we have carried out further theoretical studies.

AIM Study. We have also used Bader's theory of "atoms in molecules" (AIM),[34] which has been widely used to characterize a great variety of interactions.[58] AIM[35] calculations were done using the ab initio wave functions computed at the MP2 level of theory for complexes **c3** and **c4**. AIM theory takes the electron density (ρ) as the starting point. The interaction between any two atoms in the system is characterized by the parameters associated with the electron density at the BCP. The shortest gradient path connecting the two nuclei and the BCP represents a bond path. In terms of topological analysis of the electron density, these CPs and bond paths give rise to a molecular graph, which is a good representation of the bonding interactions. Figure 10 shows the molecular graphs for **c3** and **c4** obtained using the wave functions computed at the MP2 level. The results that are summarized in Table 10 give some helpful information regarding the strength of the noncovalent interactions involved in the complexes. It has been demonstrated that the value of the electron charge density at the CPs that are generated in anion$-\pi$ complexes can be used as a measure of the bond order.[15c]

For complexes **c3** and **c4**, exploration of the CPs revealed the presence of two BCPs that connect the anion with the pyrimidine ring via the C7 atom. As a consequence of the geometry of the complexes, one ring CP is also generated (see Figure 10). Generation of the BCPs supports the idea of the existence not only of an anion$-\pi$ interaction through the O4 atom of the triflate anion but also of a lone pair (lp)$-\pi$ interaction[59] through F5 as well. In fact, the magnitudes of the values of ρ and $\nabla^2\rho$ obtained for the O4 BCP are similar to those obtained for BCPs of other anion$-\pi$ complexes.[60−62]

NBO Analysis. With the aim of a better understanding of the nature of intermolecular bonding in **c3** and **c4** complexes, an NBO analysis was performed. The results thus obtained were analyzed in terms of the second-order

(56) Quiñonero, D.; Deyà, P. M.; Carranza, M. P.; Rodríguez, A. M.; Jalón, F. A.; Manzano, B. R. *Dalton Trans.* **2010**, *39*, 794–806.
(57) Quiñonero, D.; Frontera, A.; Deyà, P. M. *ChemPhysChem* **2008**, *9*, 397–399.
(58) (a) Cheeseman, J. R.; Carrol, M. T.; Bader, R. F. W. *Chem. Phys. Lett.* **1988**, *143*, 450–458. (b) Koch, U.; Popelier, P. L. A. *J. Phys. Chem.* **1995**, *99*, 9747–9754. (c) Cubero, E.; Orozco, M.; Luque, F. J. *J. Phys. Chem. A* **1999**, *103*, 315–321.
(59) Mooibroek, T. J.; Gamez, P.; Reedijk, J. *CrystEngComm* **2008**, *10*, 1501–1515.
(60) Quiñonero, D.; Garau, C.; Frontera, A.; Ballester, P.; Costa, A.; Deyà, P. M. *Chem. Phys. Lett.* **2002**, *359*, 486–492.
(61) Estarellas, C.; Quiñonero, D.; Frontera, A.; Ballester, P.; Morey, J.; Costa, A.; Deyà, P. M. *J. Phys .Chem. A* **2008**, *112*, 1622–1626.
(62) Escudero, D.; Frontera, A.; Quiñonero, D.; Deyà, P. M. *J. Comput. Chem.* **2009**, *30*, 75–82.

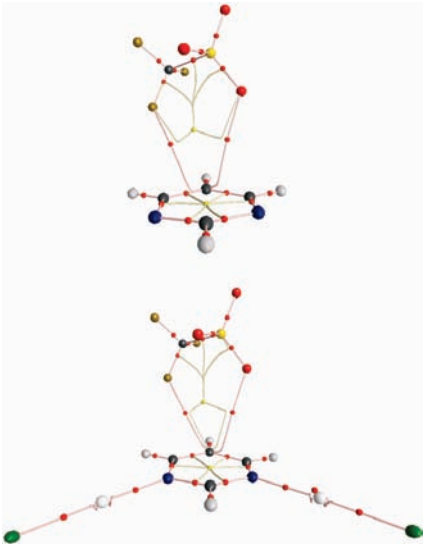

Figure 10. Molecular graphs for **c3** (top) and **c4** (bottom) computed at the MP2/AVDZ//RI-MP2/AVTZ level. BCPs are depicted in red and ring CPs in yellow.

Table 10. Electron Charge Density (ρ in au) and Its Laplacian ($\nabla^2\rho$ in au), Computed at the BCPs for Complexes **c3** and **c4** at the MP2/AVDZ//RI-MP2/AVTZ Level of Theory

compound	interacting atom	$10^3\rho$	$10^2\nabla^2\rho$
c3	O4	7.842	2.668
	F5	4.828	2.034
c4	O4	8.017	2.580
	F5	5.314	2.319

perturbation theory of the Fock matrix on an NBO basis, as shown in Table 11. Second-order perturbation theory in NBO gives the energy lowering obtained when electrons from partially occupied orbitals are allowed to delocalize into partially empty orbitals. A large energy implies a huge tendency toward delocalization and, therefore, it can be used as an indicator of electron movements. Only selected intermolecular interactions (greater or equal to 0.05 kcal mol^{-1}) are listed in Table 11 because they are the only ones of interest for our study. The second-order perturbative estimates of donor−acceptor interactions indicate that the strongest stabilization, when pyrimidine acts as a donor molecule, comes from lpN3 to O4 and S2 Ry orbitals and from lpN4 to S2 and F5 Ry orbitals. When the triflate anion acts as a donor molecule, the strongest interactions are established between lpO4 and the π-antibonding orbitals of N3C6 and C7C8. In addition, there are other minor contributions coming from interaction of lpF5 with the σ^* C6C7 and C8N4 orbitals and the π^* C7C8 orbital.

All of these results are consistent with the existence of an anion−π interaction between the triflate anion (by means of the O4 atom) and the pyrimidine ring and with the existence of an lp−π interaction between the F5 atom and the aromatic system, as was also suggested by the AIM results.

Conclusions

Functionalized tetracationic grids with four NH_2 groups located in the two open voids were built by self-assembly,

Table 11. Selected Second-Order Perturbation Theory Interactions in Complexes **c3** and **c4**[a]

donor	acceptor	**c3**	**c4**	donor	acceptor	**c3**	**c4**
π_{C7C8}	Ry_{F5}	0.06		π_{N4C9}	Ry_{F5}		0.05
	σ^*_{C32F5}		0.07	lp_{O4}	π^*_{N3C6}	0.60	0.69
σ_{C7H7}	Ry_{F5}	0.14	0.12		π^*_{C7C8}	0.75	0.81
lp_{N3}	Ry_{O4}	0.05	0.68		Ry_{N3}		0.05
	Ry_{S2}		1.55		Ry_{H7}		0.10
	Ry_{C32}		0.08	lp_{F5}	σ^*_{C6C7}		0.06
lp_{N4}	Ry_{O4}		0.18		π^*_{C7C8}	0.05	0.07
	Ry_{S2}		0.59		σ^*_{C8N4}	0.07	0.09
	Ry_{C32}		0.06		Ry_{H7}	0.05	0.07
	Ry_{F5}		0.37				

[a] Equilibrium distances R_H and R_F from H and F to the ring plane, respectively. Variation of the equilibrium distances with respect to the corresponding binary complexes (ΔR_H and ΔR_F, in Å).

starting from copper(I) salts and 2-amino-4,6-bis(pyrazol-1-yl)-pyrimidine or 2-amino-4,6-bis(3,5-dimethylpyrazol-1-yl)-pyrimidine ligands. The effect of the amino group was compared, both in the solid state and in solution, with that of H or Me groups present in other new or previously described grids. In the solid state, the grids, whose faced ligands are divergent, are receptors of different anions and two of them are located inside the two open voids of the structure. The counteranions interact with the walls of the grid through hydrogen bonds and anion−π interactions. The presence of the amino groups exerts a clear influence over the disposition of the anions inside the cavity and also the ligand orientation. The influence of the NH_2 groups is mainly due to the formation of four hydrogen bonds per void, always involving three atoms of the anions.

Experiments of anion exchange in the solid−liquid interface have demonstrated that the counteranions can be exchanged. The crystallinity of the samples is mostly preserved after an exchange process, but the crystalline structure changes. Unfortunately, the selectivity toward anions such as PF_6^-, BF_4^-, and OTf^- is low.

According to the NMR and UV−vis studies carried out, the grid structure is preserved in acetone and dichloromethane solutions. As an exception, complex **15**, with Cl^- as the counteranion, exhibits a high degree of dissociation and free ligand is present in these solutions.

The study of the diffusion coefficients (DOSY experiments) allows the conclusion that there exists a cation−anion interaction in solution but with an interchange process. From the calculated fraction of bound anion, it is deduced that the presence of amino groups in the grids has a decisive influence on the stability of the host−guest complexes, although the presence of counteranions that can give rise to stronger interactions also favors association.

The experiments of anion interchange in solution followed by ^1H and ^{19}F NMR indicated that a higher stability is found for the aggregates with OTs^- and NO_3^-. While for these anions a 1:2 stoichiometry is reached (Job plot), for the rest of the anions tested, only weaker 1:1 complexes are formed. According to the amino resonance chemical shift, the hydrogen bond strength in the cation−anion interaction follows the order $OTs^- > NO_3^- > ReO_4^- > BF_4^- \approx OTf^- > PF_6^-$.

The presence in the triflate complex **18** of an anion−π interaction whose existence, based on geometrical parameters, was uncertain and also an lp−π interaction involving a F atom have been demonstrated.

In summary, the clear effect of the amino functionality in enhancing anion binding by these tetrametallic grids in both the solid state and in solution has been demonstrated.

Acknowledgment. This work was supported by the MICINN of Spain (Grants CTQ2008-03783/BQU and CTQ2008-00841/BQU), the Junta de Comunidades de Castilla—La Mancha−FEDER Funds (Grant PCI08-0054), and Durham University. D.Q. thanks the MICINN for a "Ramón y Cajal" contract. The authors acknowledge Juan Pedro Andrés for recording the powder X-ray diffractograms.

Supporting Information Available: X-ray crystallographic files in CIF format, X-ray powder diffractograms, NMR spectra for the titrations of **6** with different salts, and a Job plot of **6** for the addition of TBA(OTs). This material is available free of charge via the Internet at http://pubs.acs.org.